UTILIZATION OF MICROBUBBLES FOR ENHANCEMENT OF OXYGEN TRANSFER IN XANTHAN FERMENTATION

By

BANGALORE DHARMENDRA

Master of Science

In

Dairying [Dairy Engineering]

National Dairy Research Institute,
Karnal, India

2000

Submitted to the Faculty of the
Graduate College of the
Oklahoma State University
In partial fulfillment of
the requirements for
the Degree of
MASTER OF SCIENCE
August, 2003

UTILIZATION OF MICROBUBBLES FOR ENHANCEMENT OF OXYGEN TRANSFER IN XANTHAN FERMENTATION

Thesis Approved:

Daniell Bellmer

Thesis Advisor

Randy S. Lewis

Glenn Krenzler

Timothy J. Pettitone

Dean of the Graduate College

ACKNOWLEDGEMENTS

It has been a privilege to express my profound sense of gratitude to Dr. Dr.Danielle Bellmer, for her guidance, encouragement, valuable suggestions, support, and patience throughout the study.

My sincere thanks to the members of advisory committee: Dr. Randy Lewis for his advises and suggestions throughout this project, and in specific his biochemical engineering course, which helped me, get a better insight into the concepts for my research, Dr.Glenn Kranzler for his guidance, encouragement and patience in editing my thesis. I also owe my thanks to Shekar patel for having helped me through out my research both in understanding my project and conducting my experiments.

I am also thankful to Dr. Sigfusson and Renne Albers-Nelson for their technical expertise and assistance in conducting my experiments on particle size analyzer. Thanks to Biosystems Engineering department for supporting my education, and Food and Agricultural Products Research Center for carrying out my research and all other staff involved in center for having helped me in various disciplines.

Sincere thanks to all friends and my loving gratitude to my parents for having made me what I am today.

TABLE OF CONTENTS

LIST OF FIGURES

LIST OF TABLES

CHAPTER I

INTRODUCTION

Xanthan gum is one of the most important industrial microbial polysaccharides. Its rheological and stabilizing properties make it a potential ingredient in a wide range of applications. This biopolymer is synthesized as a capsule/slime on Gram-negative *Xanthomonas Campestris* during an aerobic fermentation process that lasts between 60 and 90 hours. The commercial production of xanthan gum is an expensive process due to high operational costs incurred mainly from air processing, agitation, and downstream processing. The viability of this process is hence dependent on maximum productivity during the fermentation process. Considerable progress has been made through genetically engineering strains, improvements in the design of fermenters and impellers in particular, optimizing operating variables such as air flow rate, temperature, pH, etc., and medium standardization to improve the process economics. However, to realize these benefits from the above developments, it also becomes necessary that an effective mass transfer system be incorporated.

The importance of mixing is related to the mass transfer coefficient, which is considered to be an important index for optimizing a fermentation process. Since xanthan gum production is an aerobic fermentation process, oxygen becomes one of the essential nutrients to facilitate the growth of microorganisms. Oxygen input generally involves sparging air from the bottom of the fermenter. Sparging generates bubbles that traverse to the surface of broth, because they are less dense than the substrate used for fermentation. During this process,

oxygen from the gas bubble is exchanged with the microorganism and the efficiency of mass transfer, expressed as the mass transfer coefficient, becomes a vital factor in determining the efficiency of the fermentation process. Further xanthan fermentation involves a characteristic shift in broth viscosity due to the synthesis of the xanthan on the surface of microorganisms in the form of slime that is later released into the fermentation medium. It therefore becomes necessary that proper mixing and mass transfer be ensured to achieve high xanthan gum yields. Increasing the agitation rate was considered to be an effective way of achieving improvements in mixing. However, it has been realized that an increase in agitation rate achieved by increasing impeller speeds would mean an increase in power consumption due to fact that power incurred is proportional to the third power of impeller speed (N^3) and the fifth power of impeller diameter (D^5). Further, the shear-sensitive nature of microorganisms becomes a limiting factor for higher agitation speeds. Therefore, studies are underway to find alternative means of increasing the efficiency of fermentation processes.

An alternative approach for increasing the mass transfer rate could be the application of microbubbles in the fermentation processes. Microbubbles are surfactant-stabilized spherical bubbles generated by mixing surfactant solutions (anionic, cationic, or nonionic solutions) at relatively high speeds over a period of time. These bubbles are on the order of 10-100 μm in diameter in comparison to 3-5 mm bubbles caused by conventional air sparging in fermenters. Some important properties of microbubbles include increased interfacial area per unit

volume as a result of small size and gas hold-up, high stability, ease of conveyance through pumps without collapse, and ease in separation of aphron phase from bulk liquid phase (Jauregi and Varley, 1999). The smaller size of bubbles also ensures more complete utilization of oxygen (up to 95%) from these microbubbles than what is achievable in conventional air sparging. With air sparging, oxygen goes incompletely utilized in the bioreactor due to poor solubility of oxygen in aqueous media and quick rising to the surface because of large bubble size leading to coalescence. These properties have enabled diverse applications for microbubbles in areas like protein recovery, bioremediation, predispersed solvent extraction of dilute products, flotation for removal of biological and non-biological products, enhancement of mass transfer in two-phase systems for enzyme extraction, enhancement of mass transfer in three-phase systems for microbiological fermentations, and other applications (Jauregi and Varley, 1999).

Some researchers have investigated the application of microbubbles for enhancement of mass transfer, and results have been found to be encouraging. The increase in mass transfer has been explained by an increase in interfacial area (a), which is a function of bubble size causing an increase in mass transfer rates in bioreactors. This is alternatively termed the volumetric mass transfer rate (K_La), which is a product of the mass transfer coefficient, K_L, and the interfacial area, a. Studies involving the application of microbubbles in yeast fermentation (Pramuk, 2000) and synthetic gas fermentation (Bredwell and Worden, 1998) have resulted in a four- to six-fold increase in volumetric mass transfer rate

values causing increased growth rates of microorganisms in comparison to conventional air sparging in bioreactors. This result has led to an interest in investigating similar advantages for xanthan gum fermentation systems to achieve increased yield and reduce the energy cost incurred in agitation.

The main objectives of this research include:

- Evaluate and optimize the properties of generated microbubbles
- Study biomass and xanthan yield patterns at step-agitation conditions for both air and microbubble sparging
- Study the effect of microbubbles on the oxygen uptake rate and oxygen transfer rate based on dynamic gassing out technique
- Compare the energy consumption in air and microbubble sparging systems

CHAPTER II

REVIEW OF LITERATURE

Polysaccharide production in early years was from higher plants and seaweeds. The abundance of cornstarch and the large market for water-soluble gums led to an interest in alternative sources of gums. In the 1950's, scientists at the Northern Regional Research Laboratory of USDA investigated microorganisms that could biosynthesize water-soluble gum products to supplement the existing natural water-soluble gums. The result of this research was identification of the *X. Campestris* species that could produce xanthan gum with unique properties. An important aspect was the relatively high conversion rates achievable from these fermentation processes. It was found that Xanthomonas organisms could convert up to 70% of the carbohydrate substrate (glucose) to exopolysaccharides. Later in the 1960's, KELCO carried out pilot scale studies of xanthan and with extensive research developed procedures leading to commercial production in 1964. Kelco started marketing xanthan with the trade name KELTRAL for food grade xanthan and KELZAN for industrial grade xanthan. Development of xanthan was catalyzed with the approval of US-FDA after toxicological and safety studies permitting its use in food products without specific quantity limits. FDA and USDA jointly permitted the use of xanthan as an ingredient in a wide range of food applications and paper-based packaging materials used for food applications. Xanthan received approval by the United States Environmental Protection Agency (EPA) for use as an inert ingredient in pesticide formulations. Application of xanthan for enhanced oil

recovery based on the principle of micellar/microemulsion flooding is also a potential application that has been investigated for the oil industry. Similar approval from other regulatory agencies across the world increased the importance of xanthan, and today we find across the globe a plethora of applications for xanthan and a large number of companies commercially producing xanthan gum.

Xanthan Gum

Xanthan gum is an anionic exocellular heteropolysaccharide produced by the genus Xanthomonas. Of the various microorganisms investigated under this genus, the *X. Campestris* species is reported to yield a polymer with unique properties (Kennedy and Bradshaw, 1984). The structure of xanthan gum is shown in Figure1, and it can be seen that a series of repetitive structural units forms the xanthan molecule, giving it specific unique properties. Its properties include high molecular weight (about 2-20 million Daltons), pseudoplastic nature, high apparent viscosity at low concentrations and stability within wide ranges of pH, pK (ionic concentration) and temperature that could be attributed to the molecular structure and confirmation in solutions. This has led to its extensive application in food, cosmetic, paper and textile, pharmaceutical, and oil industries as a stabilizing, thickening, emulsifying, gelling, and suspending agent (Kennedy and Bradshaw, 1984; Cottrell and Kang, 1978; Galindo, 1985; Pace, 1987).

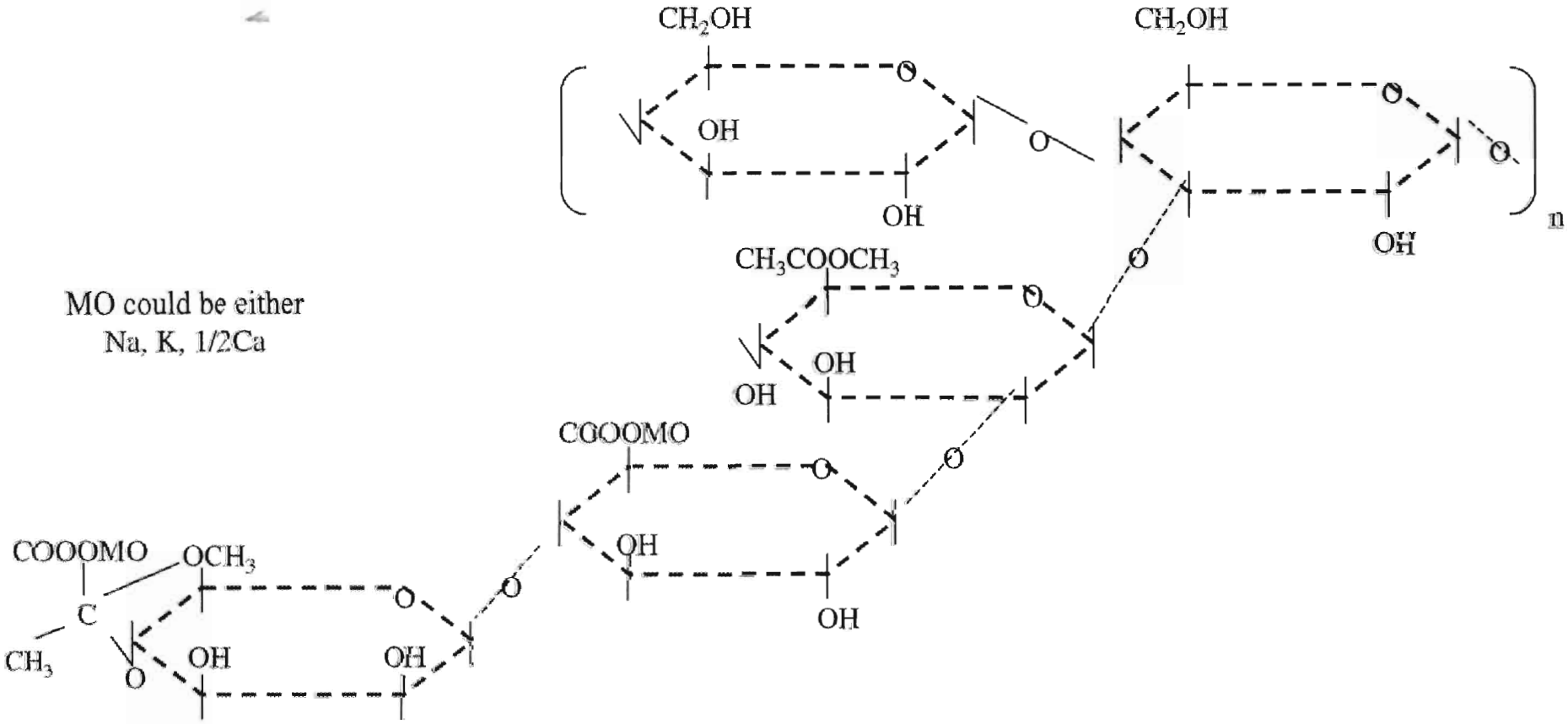

Figure1. Structural formula of xanthan gum

Xanthan Gum Production

Xanthan gum production involves a batch aerobic fermentation process wherein xanthan is synthesized as a capsule (Kennedy and Bradshaw, 1984) by the *X. Campestris* species. Typically, sucrose and whey are utilized (Atkinson and Mavituna, 1991; Liakopoulov-kyriakides et al., 1997) as the substrate within the fermentation medium, and the process lasts up to 80 hours (Kennedy and Bradshaw, 1984). A flow diagram (Moraine and Rogovin, 1973) for the xanthan gum production process is shown in Figure 2 (Albrecht et al., 1963). The unique properties of xanthan are offset by complications in mixing caused by rheological changes in the fermentation media due to a phase shift from newtonian to non-newtonian behavior. This result makes the process one of the most complicated among industrial aerobic fermentation processes (Margaritis and Pace, 1985). This phase shift can be attributed to the production of extracellular polysaccharide, which keeps accumulating, causing rheological complexities leading to cavern formation and possibly stagnant regions due to insufficient mixing (Amanullah et al., 1998). The problems in mixing result in reduced oxygen transfer rates causing low microbial oxygen uptake and thus a decrease in final xanthan yields. Rogovin et al. (1961) was the first to report the problem of poor bulk mixing and reduced oxygen transfer rates in the xanthan gum fermentation process. Since then, considerable work has been done to address the problem (Rogovin et al., 1961; Funahashi et al., 1987b; Funahashi et al., 1988a, Funahashi et al., 1988b, Nienow, 1984; Peters et al., 1989; Peters et al., 1992; Soloman et al., 1981a) and has been concluded that these two factors are critical

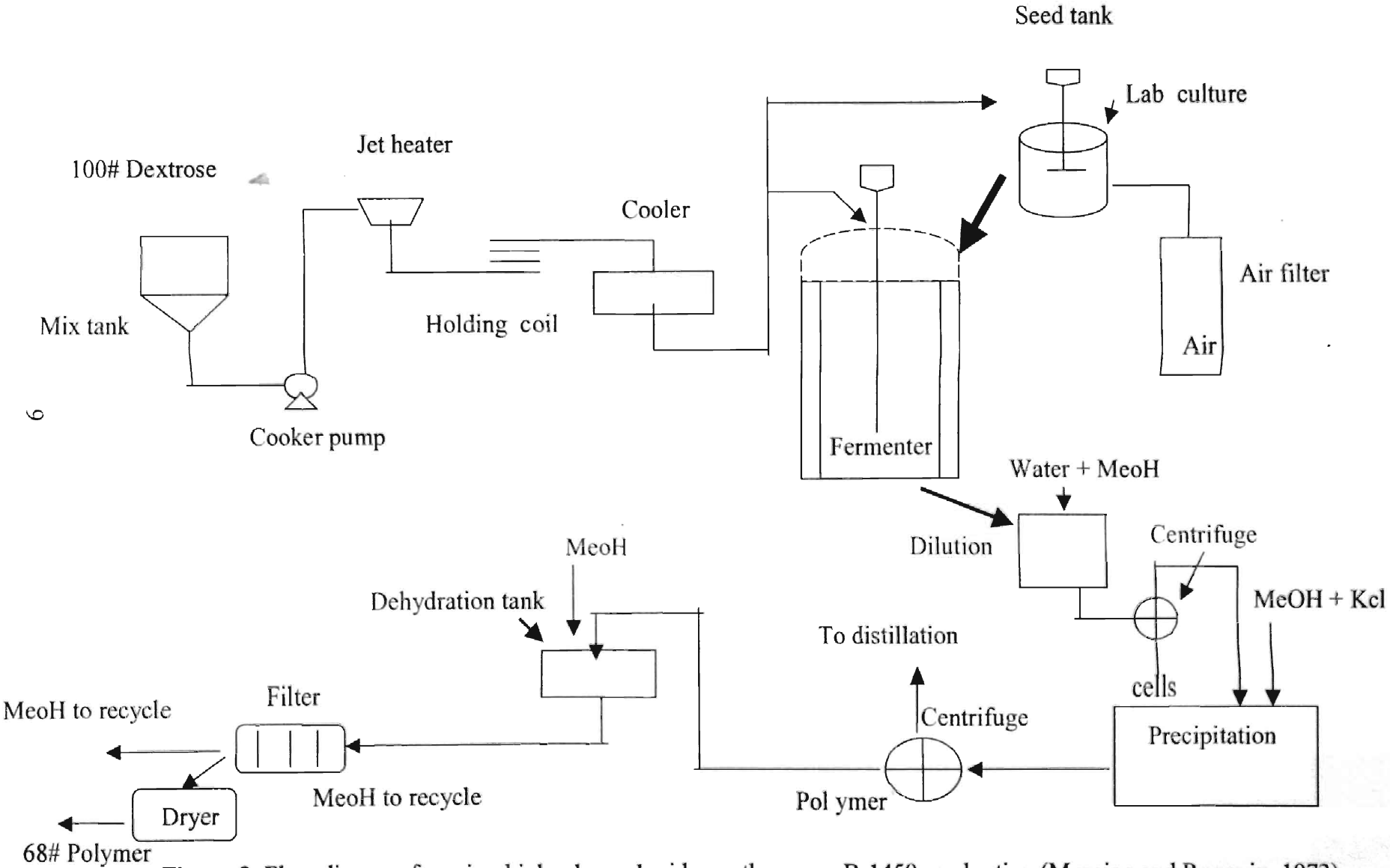

Figure 2. Flow diagram for microbial polysaccharide xanthan gum B-1459 production (Moraine and Rogovin, 1973)

in determining the productivity of xanthan gum fermentation processes. Equally important are other non-process variables such as cultivation procedures (Funahashi et al., 1987a), bacterial strain (Marquet et al., 1989), culture media (Souw and Demain, 1979), feeding methods (Peters et al., 1992; De Vuyst et al., 1987) and process variables such as pH (Moraine and Rogovin, 1971), temperature (Shu and Yang, 1990), and dissolved oxygen (Suh et al., 1990), which have been extensively investigated. Galindo (1994) and Pace and Righelato (1980), reported that the viability of xanthan gum production is also very dependent on downstream processing costs, and so it becomes necessary that at least about 25g/L of xanthan yield is achieved within the xanthan gum production process in order for it to be economical. A list of studies involving xanthan fermentation carried out with a wide range of operating conditions have been tabulated elsewhere (Amanullah et al., 1998). While the problems of mixing has been addressed through improved vessel and impeller design (Fletcher, 1994), use of double impellers (Nokajim et al., 1990) and optimizing the process variables (Nokajim et al., 1990; Funahashi et al., 1987a; Funahashi et al., 1988), the problem of oxygen mass transfer has been of continued interest to researchers.

Oxygen Mass Transfer in Xanthan Fermentation

The aerobic xanthan fermentation process involves growth of *X. Campestris* microorganisms leading to xanthan gum production. To achieve optimal growth rates of the organism, it becomes necessary that nutrients be

facilitated in optimum amounts. While nutrients that are soluble in water do not pose a problem, water insoluble nutrients such as oxygen are often critically limiting. Stanbury et al. (1995) reported that in liquid media the solubility of oxygen is about 6000 times lower than glucose, and can decrease further due to temperature rise and the presence of other nutrients in the broth. It therefore becomes necessary that oxygen supplied to the fermenter be effectively utilized for optimum cell and/or product formation through appropriate aeration and agitation. Oxygen is generally introduced into the fermenter by sparging air into the bottom of the fermenter, which is termed as aeration. Agitation actually refers to the mixing of air bubbles in the medium with the help of an impeller driven by an electric motor. The process of agitation also enables the breaking of large bubbles into small bubbles, thereby facilitating uniform distribution of air bubbles within the medium. Oxygen, once introduced as air bubbles into the fermenter, diffuses from the gas bubble through the (1) gas-liquid interface, (2) stagnant region, (3) bulk liquid, (4) stagnant region around cell, (5) liquid layer around cell, (6) finally through the cell membrane into the reaction site (7-9) as shown in Figure 3 (Bailey and Ollis, 1986). The rate of oxygen diffusion/transfer by the above mechanism can be defined by the equation:

$$N_A = K_L a \Delta C \quad \ldots\ldots(1)$$

Where:

N_A = oxygen transfer rate/unit volume of fluid (mol $m^{-3}s^{-1}$)

K_L = liquid phase mass transfer coefficient (ms^{-1})

a = gas liquid interfacial area per unit volume of fluid (m^2m^{-3}) and

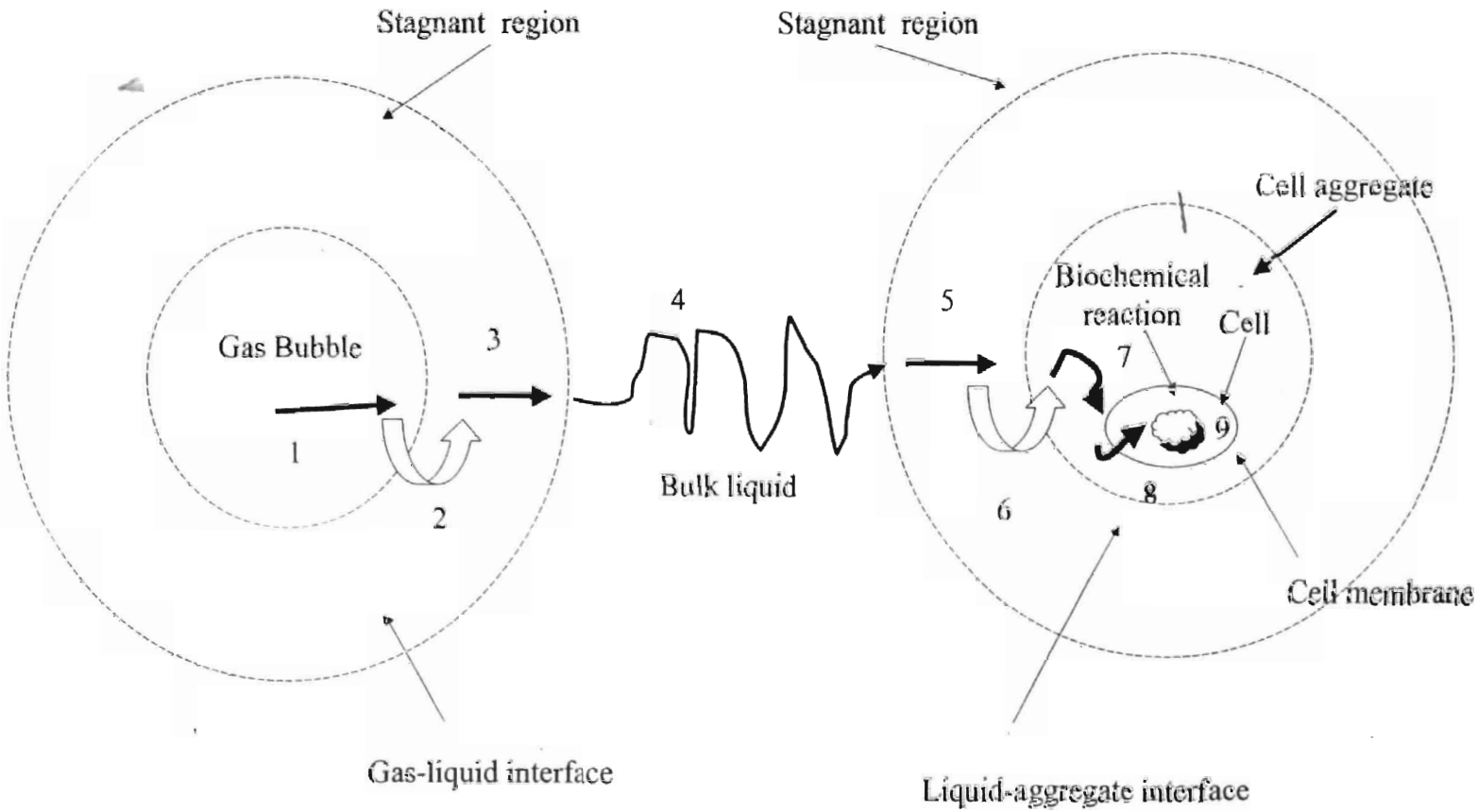

Figure 3. Schematic representation of oxygen transfer from a gas bubble to inside a cell (Bailey and Ollis, 1986)

ΔC = C*-C., concentration driving force (mol m^{-3}), which is the difference between C* (saturated dissolved oxygen concentration) and C (oxygen concentration in liquid medium).

The oxygen mass transfer rate is affected by several factors: interfacial area of the gas bubble; bioreactor geometry (inclusive of vessel, stirrer, and distributor design); liquid properties like surface tension, viscosity, dissipated energy in fluid in terms of air input and impeller speed; medium composition; presence of antifoam agents; temperature during fermentation; oxygen partial pressure, and medium properties that change over time (Garcia-Ochoa et al., 2000; Doran, 1995; Richard, 1961). Oxygen mass transfer is generally represented by the volumetric mass transfer coefficient which is the product of K_L and a (neglecting C*-C which is relatively small and due to the low solubility of oxygen). The product K_La becomes an important factor in scale-up and design of fermentation systems. An approach to evaluate K_La values has been use of either experimental correlations that establish a relation between K_La and stirrer speed (P/V), superficial air velocity, apparent viscosity for non-newtonian fluids (Dussap et al., 1985; Linek and Vacek, 1988; Tecante and Choplin, 1993; Garcia-Ochoa and Gomez, 1998) or empirical correlations which are based on dimensionless numbers (Garcia-Ochoa and Gomez, 1998; Yagi and Yoshida, 1975; Nishikawa et al., 1981). Although these correlations estimate K_La values, their suitability becomes system- and process-specific, and a much better approach would be to use methods developed for oxygen transfer rate measurements in a bioreactor. Several known methods exist, including the yield

coefficient method, dynamic method, sodium sulfite oxidation method, and the direct method. Pramuk, 2000 has given a detailed description of these methods, the advantages and disadvantages they offer, and suitability of the individual methods for particular operating conditions. The general principle of these methods is as follows. The yield coefficient method relates oxygen and cell mass kinetics stoichometrically to measure the oxygen uptake rate by the microorganisms (Moser, 1966). The dynamic method is based on unsteady state mass balance relations for oxygen in a fermenter (Taguchi and Humphrey, 1966). The sodium sulfite oxidation method uses the principle of oxidation of sodium sulfite to sodium sulfate with copper as catalyst to measure the oxygen transfer rate in the fermenter (Cooper et al., 1944). The direct measurement method measures the oxygen concentration difference between air inlet and exit of the fermenter (Wang et al., 1971) to derive information on the mass transfer properties in the fermenter.

Microbubble Technology

Sebba (1971) reported that surfactant solutions, when subjected to intense stirring (5000-10000 rpm) cause gas entrainment and microbubble formation. The bubbles generated through this means were on the order of 10-100μm in diameter relative to the colloidal range (1nm-1μm) (Shaw, 1992), and so they were also referred to as colloidal gas aphrons (CGA). Kaster et al. (1988) termed it as microbubble dispersion because of a combination of small size (20-70μm) and large size bubbles (3-5 mm) produced by his CGA generator. This combination was achieved with a CGA generator (Figure 4) developed by

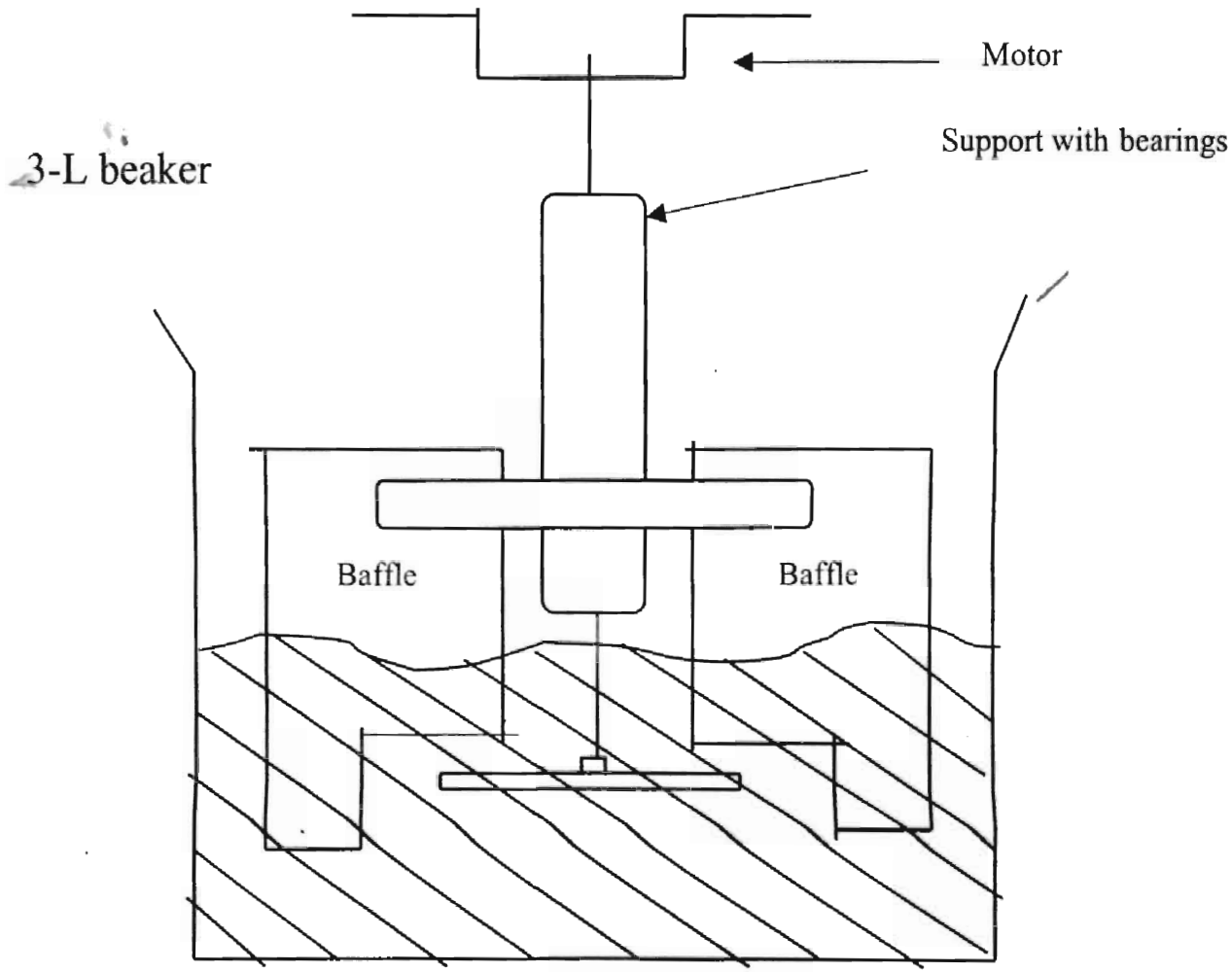

Figure 4. Spinning Disc CGA Generator (Sebba,1985)

Sebba (1987), which was an improved version of his original microfoam generator (Sebba, 1971). The system consisted of a horizontal disk ~ 5cm in diameter submerged in a surfactant solution at about 2-3cm containing baffles to obtain the desired mixing range (Sebba, 1985). Various combinations of ionic, cationic, and non-ionic surfactants have been investigated for CGA generation, and microbubble properties assessed with reference to several applications have been reviewed (Jauregi and Varley, 1999). The characteristics of CGA are as follows: large interfacial area per unit volume a ($a=6\varepsilon/d$) attributed to small bubble size (d) and high gas holdup (ε), relatively high stability due to a soapy shell surrounding the gas core delaying coalescence, easy to convey feature without collapse, and quick separation of the aphron phase from the liquid phase. These unique properties can be attributed to the structure of the microbubble (Figure 5) in comparison to conventional air-sparged bubbles. The surfactant-stabilized bubble consists of an inner gas core covered by a surfactant shell that separates the inner gas core from the outer bulk liquid phase. The properties associated with microbubbles have been defined as follows:

a) Stability or half life (τ): generally defined as the time taken for half of the initial liquid to separate from the foam once stirring ceases.

b) Gas hold-up: The extent of air incorporated expressed as a ratio of gas entrained after and before mixing. This parameter can be calculated by measuring the heights or volumes in microbubble generator before (V_{ao} and h_{io}) and after mixing (V_g and h_o) using the following equation: $\varepsilon_o=V_g/V_{ao} = (h_0-h_{i0})/h_0$

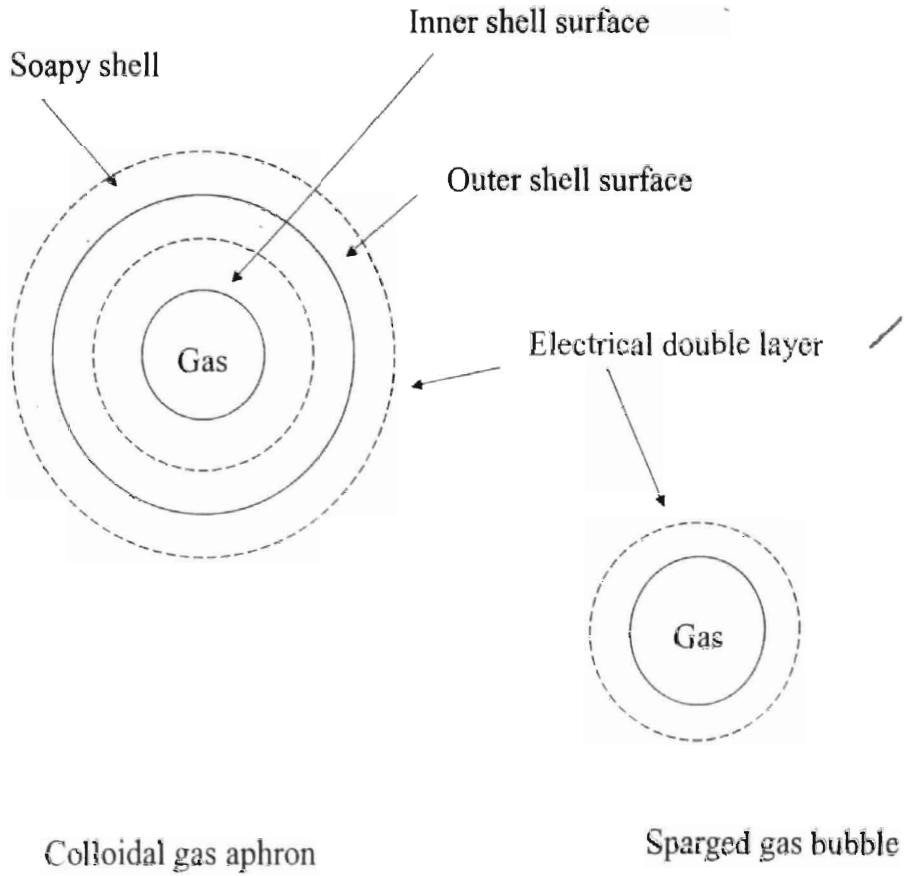

Figure 5. Colloidal gas aphron and sparged air bubble structure (Kaster, 1988)

c) Aphron diameter: refers to diameter (d) of microbubble measured by microscopy and image analysis (Save and Pangarkar, 1994; Jauregi et al., 1997) or laser techniques (Chapalkar et al., 1993; Bredwell et al., 1995; Roy et al., 1992; Kommalapati et al., 1996).

These properties are dependent upon the operating parameters such as surfactant concentration, speed of stirring, time of stirring, and surfactant type. Reports state that maximum stability (Save and Pangarkar, 1994; Jauregi et al., 1997; Chapalkar et al., 1993; Matsushita et al., 1992; De Vries, 1972), high gas hold up (Jauregi et al., 1997; Chapalkar et al., 1993; Kommalapati et al., 1996; Matsushita et al., 1992), and smaller bubble sizes (Save and Pangarkar, 1994) result at concentrations above critical micelle concentration [CMC] (the concentration above which micelle formation becomes appreciable) for a particular surfactant. An increase in surfactant concentrations beyond this concentration would result in larger bubble sizes. Investigations involving the effect of speed of stirring on microbubbles have resulted in establishing a critical limit of 5000 rpm for CGA generation (Nishikawa et al., 1981; Jauregi et al., 1997; Chapalkar et al., 1993; Matsushita et al., 1992). Stability studies on CGA have varied reports, with some researchers stating that ionic surfactants yield more stable dispersions in comparison to non-ionic surfactants (Matsushita et al., 1992), and stability further increases with an increase in alkyl chain length (Save and Pangarkar, 1994). Chalpalkar et al. (1993) reported that the type of surfactant had no effect on stability, but gas hold-up increases were reported for non-ionic compared to ionic surfactants. However, Bredwell et al. (1995) reported

no effect of surfactant type on gas hold-up. Increases in gas hold-up were reported for increases in time of stirring (Jauregi et al., 1997; Matsushita et al., 1992).

Microbubble Approach in Fermentation Systems

Fermentation processes are gas-liquid mass transfer limited. The approach widely practiced and reported to address the problem is by increasing the impeller speed. However, increasing impeller speed increases power consumption, because power consumption is proportional to the third power of impeller rate and the fifth power of impeller diameter (Bailey and Ollis, 1986). This increase would not only make the process cost-intensive because of high energy inputs, but could also prove detrimental to the shear-sensitive nature of microbial cells. Although this approach enabled an increase in the K_L value (Equation 1), the extent achievable is a function of bubble size. Doran 1995 reported that K_L increased with agitator speeds up to bubble sizes of 2-3mm, after which it was observed to be insensitive to any changes in fermenter process conditions. It therefore becomes imperative to investigate alternative approaches for increasing mass transfer through increases in interfacial area, which is inversely related to gas bubble size. MortarJemi and Jameson (1978) reported that for effective oxygen utilization in mass transfer applications, there is a need for developing bubble sizes in the range of 100-300μm.

Microbubbles and their unique properties show great potential to increase volumetric mass transfer coefficients and hence mass transfer efficiency.

Microbubble sparging was reported to yield higher K_La values in comparison to ordinary air sparging during a sodium sulfite oxidation experiment conducted by Wallis et al. (1986). Worden and Bredwell (1998) reported that microbubbles could facilitate a 10,000-fold increase in mass transfer rate in comparison to conventional air bubbles. The application of microbubbles in fermentation processes has been investigated in yeast & synthesis gas fermentation (Pramuk, 2000; Kaster et al., 1990; Bredwell and Worden (1998); Hensirisak, 1997). The property of being easy to convey without collapse enables generation of microbubble at one end and then pumping them to the fermenter. Kaster, 1990 reported a four-fold increase in K_La values during aerobic fermentation of yeast cells *Saccharomyces Cerevisiae* with microbubble sparging relative to air sparging in a 1-liter fermenter. Bredwell and Worden, 1998 studied the mass transfer properties of microbubbles in synthesis gas fermentations in comparison to air sparing and reported K_La values of $14h^{-1}$ for air sparging and $91h^{-1}$ for microbubble sparging. Pramuk, 2000, also reported an increase in yeast cell growth due to increase in K_La values with microbubble sparging. His experiment consisted of a 1-liter fermenter that was later scaled up to 50-liter capacity. Similar increases in K_La values were observed.

It was further inferred that the same cell yield was achieved at 150 rpm with microbubble sparging as that obtained by ordinary air sparging at 500 rpm, thus resulting in a 3-fold reduction in energy consumption to achieve the same biomass yields. Similar results involving increased mass transfer were observed by Hensirisak (1997). Total energy consumption savings were estimated to be

68% and 55% with microbubble sparging at 150 rpm for 50- and 20-liter fermenters compared to that achieved at 500 rpm with conventional air sparging. This result also is an indication of larger benefits that could be achieved with scale-up of these fermenters. Since fermentation processes involve microorganisms, it becomes necessary that surfactants and concentration levels should not affect growth of microorganisms, but at same time surfactants need to generate microbubbles with good properties. Bredwell et al. (1995) investigated the formation and coalescence properties of microbubbles and reported that Tween-20, a non-ionic surfactant, would be suitable for fermentation processes. Bredwell et al., 1997 also reported that Tween-20 is biocompatible with *Butyribacterium methylotrophicum* at concentrations of twice the CMC level (120 mg/l).

The results from the above studies on the potential microbubbles offer in fermentation processes could equally be explored for xanthan gum fermentation for increasing growth of microorganisms by enhancing oxygen mass transfer and yielding high xanthan concentrations, thereby improving the productivity. The present research investigates whether microbubbles are effective in increasing xanthan yield relative to air sparging, and the extent of benefit it offers in terms of savings in energy through comparative assessment.

Chapter III

MATERIALS AND METHODS

Microorganism and Strain Maintenance

The microorganism used in this study was *X. Campestris* NRRL B-1459 obtained in lyophilized state from Northern Regional Research Laboratory; U.S.Department of Agriculture (Peoria, IL). The lyophilized culture in the ampule was aseptically removed, transferred to a shake flask medium, and incubated for 48 hours at 28^0C. This procedure served as a base for producing a large number of working lyophilized cultures as bead suspensions, which were then stored at freezing temperatures. The contents of an ampule were later transferred to a shake flask medium, incubated at 28^0C for 48 hours, and then used to inoculate YMPG agar slopes that served as stock cultures for our fermentation experiments. These stock cultures were held at 4^0C in a refrigerator and transferred every 2 weeks to maintain good viability and stability for xanthan production.

Culture Media Composition and Media Preparation

The composition of medium used in our study expressed in g/L is as follows: **YMPG Slope medium**: Yeast extract-3, malt extract-3, peptone-5, glucose-10, and agar-28. **Shake flask medium**: Yeast extract-3. Malt extract-3, peptone-5 and glucose-15. **Fermentation medium**: A well-defined media based on Peters *et al.* (1989) was used as production medium. Glucose-50, citric acid-2.3, KH_2PO_4-5, NH_4CL-2, Na_2SO_4-0.114, $MgCl_2.5H_2O$-0.163, $ZnCl_2$-0.0067, $FeCl_3.6H_2O$-0.0014, $CaCl_2.2H_2O$-0.012, H_2BO_3-0.006, Na_2CO_3-0.5. The

preparation of shake flask and YMPG medium involved dissolving the media components in small amounts of distilled water while stirring in an Erlenmeyer flask on a magnetic stirrer followed by filling to desired volume by addition of remaining distilled water. In the case of production medium, glucose was sterilized separately from the rest of the components and transferred into the fermenter after cooling in order to avoid Maillard reaction.

The 5 M NaOH solutions were prepared by dissolving 200 gms of NaOH pellets in 1 liter of distilled water and mixing until completely dissolved. Saturated KCL solutions for xanthan analysis were prepared by dissolving KCL crystals in water until sediments of KCL started forming, which indicated the point of saturation. A buffer solution of sodium nitrate/sodium dihydrogen phosphate for HPLC was prepared by dissolving 17 grams of sodium nitrate and 1.56 grams of sodium dihydrogen phosphate in 1liter of distilled water and adjusting the pH to 7 before use. All above reagents were purchased from Oklahoma State University Chemistry Departmental stores.

Inoculum Preparation

Cells from stock culture were transferred to slants and incubated at 28^0C for 36 hours. About 2 loops of actively growing cells from a slant were inoculated into a tissue culture bottle containing 20 ml of shake flask medium and incubated for 24 hours at 28^0C. About 5 ml of inoculum was transferred into each of two 500-ml conical flasks containing 100 ml of shake flask medium and incubated at 28^0C for 24 hours on a rotary shaker at 150 rpm. The inoculum was later

inoculated into a lab scale fermenter containing 6-L production medium, which was equivalent to 3.33% of the fermenter volume.

Analytical Protocols

Determination of Microbubble Properties

Microbubbles were generated in a microbubble generator (Sebba, 1985) by stirring Tween-20 surfactant solution at high speed (> 5000 rpm) until a constant volume of microfoam was generated. The microbubble properties were studied over a wide range of process conditions to determine the effect of process variables and to standardize the operating parameters of the microbubble generator for actual fermentation experiments. The microbubble properties of gas hold-up and foam stability were studied for the following set of conditions:

Surfactant concentration: 120, 300, and 500 ppm

Generator speed: 5000, 6000, 7000, and 8000 rpm

Treatment time: 2, 3, 4, and 5 minutes

Gas hold-up refers to the extent of air incorporation into the dispersion and hold-up just before collapse after treatment in a particular process condition. It was measured as the ratio of volume of gas in the dispersion to the dispersed volume of surfactant solution and is given by equation:

$$\epsilon_0 = (H_0 - H_{10})/H_0 \quad \text{.....(2)}$$

Where,

ϵ_0 = Gas hold-up

H_0 = Height of final dispersion volume and

H_{10} = Height of initial surfactant volume

Stability is expressed as the time required for half of the liquid to collapse once stirring is stopped. It was measured with the help of a stopwatch. Time was reported in minutes.

Microbubble size distributions were measured on a Beckman Coulter LS 230 series particle size analyzer (Coulter Corp., Florida) that works on the principle of diffraction of laser light. The microbubble size distributions were determined at standardized conditions of the microbubble generator with solutions containing surfactant in water, surfactant in production medium and surfactant in production medium, with 0.5 and 1% xanthan levels. The module selected for our experiments was the Small Volume module with the following sequence of steps:

1. Microbubble samples were prepared in the microbubble generator.
2. Following instrument calibration, the LS particle size analyzer software was activated on and run until Obscuration = 0% was indicated.
3. Sample was loaded into the inlet port until the Obscuration indicator read OK
4. With this initiation, the particle size analyzer began profiling the particle size distribution and finally reported the average microbubble size and particle distributions within the sample. The next sample was then loaded.
5. Operational parameters: Model-Fraunhofer; run-time, 90 seconds; Obscuration - 7%; pump speed for circulation - 30 rpm; refractive index of air - 1.0008.

Interfacial area was calculated from microbubble size (assumed to be spherical) and gas hold-up using the equation: $6\epsilon_0/d$.

Determination of Microbial Counts (SPC)

Microbial plate counts (standard plate count (SPC)) were determined by subjecting the broth to deci-normal dilution to obtain dilutions on the order of 10^{-7} - 10^{-8}. Dilutions were plated on YMPG slant/agar medium on petri plates. The plated samples were incubated at 28^0C for 3 days and microbial counts enumerated.

Determination of Biomass Concentration

The biomass concentration was determined by measurement of absorbance at 565 nm using a Beckman DU series 500- spectrophotometer (Beckman Instruments, Inc.). One ml of fermentation broth was diluted 15 times with distilled water under aseptic conditions. Absorbance was measured against a reference distilled water blank, which gave the absorbance due to gum and cells ($A_{gum + cells}$). Immediately, the dilution was centrifuged (12,000 rpm for 50 min at 5^0C). The absorbance of the supernatant was measured against a reference distilled water blank giving the absorbance due to gum (A_{gum}). Actual absorbance due to cells was then expressed as:

$$(A_{gum + cells}) - (A_{gum})$$

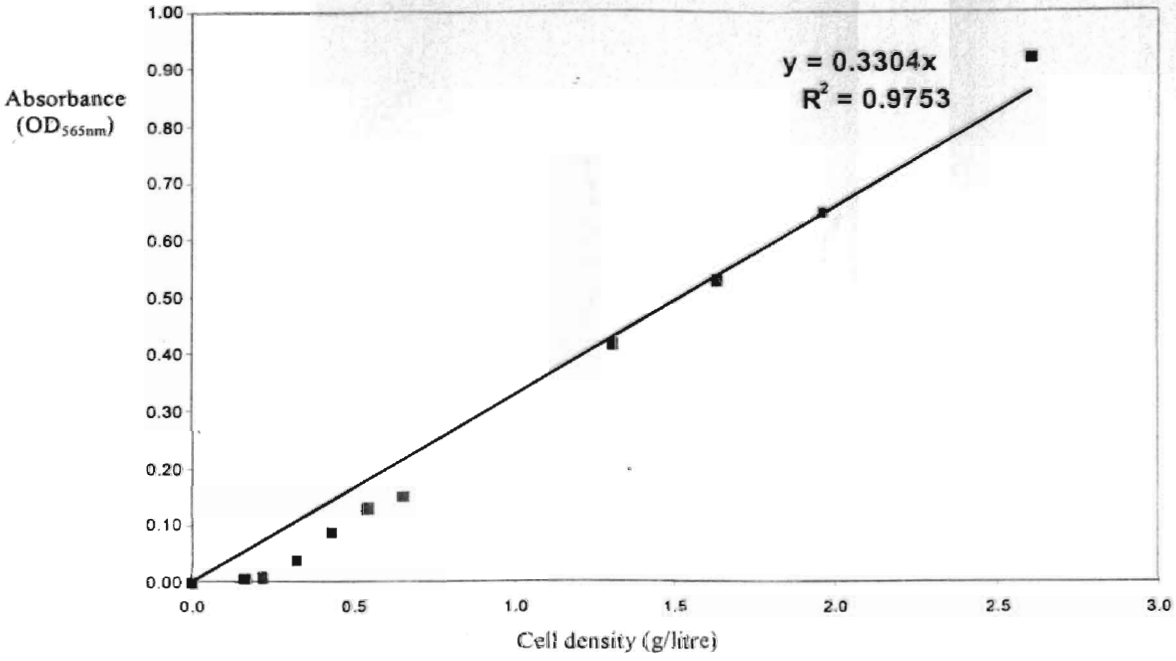

Figure 6. Cell density calibration curve

The absorbance values were then correlated with a calibration curve of OD_{565} vs. biomass concentration to obtain the actual biomass concentration. The calibration curve was prepared by growing large amounts of cells in 250 ml of broth followed by centrifugation to obtain a concentrated cell pellet. Cell pellets were later suspended in water to form a cell suspension and then diluted serially. Corresponding OD_{565} values were measured for the dilutions. This procedure resulted in a calibration curve (Figure 6) of biomass concentration vs. OD_{565} that had a regression coefficient (R^2) of 0.98.

Determination of Xanthan Concentration

Xanthan concentration was determined by the dry-weight method. This procedure involved precipitation of cell-free supernatant with 2 volumes of isopropyl alcohol and 5% of total volume of freshly prepared saturated KCL

solution followed by centrifugation at 12,000 rpm for 40 min. The pellet/precipitate was then collected and dried overnight at 105^{0}C to determine xanthan concentration.

Determination of Xanthan Molecular Weight

Xanthan molecular weight was determined using high-pressure liquid chromatography (HPLC) on a 2xPL aquagel-OH 60 15 µm, 300 x 7.5 mm column, which was able to detect molecular weights in the range suitable for xanthan analysis. The eluent used was 0.2 M $NaNO_3$ / 0.01M NaH_2PO_4, pH 7 at a flow rate of 1ml/min. Commercial xanthan gum from Sigma chemicals was used to prepare a 0.01% xanthan solution to run standards. The detector used was a refractive index detector (Waters-410 Differential Refractometer, Waters Corporation, Milford, MA). A sample aliquot of 100 µL was injected into the Aquagel column at ambient temperature. The procedure was conducted twice. Software used was Millennium 3.2.

Prior to molecular weight determination, xanthan samples were obtained after having precipitated the broth thrice with 2 volumes of isopropyl alcohol and 5% of total volume of freshly prepared saturated KCL solution, followed by dilution with deionized water for a concentration of 0.01%. Samples were either immediately analyzed or kept under lyophilized conditions before analysis.

Determination of OUR and K_La values

The measurement of oxygen uptake rate (OUR) and K_La was made in two stages using a dynamic gassing-out technique (Taguchi and Humphrey, 1966). The first stage involved interrupting the airflow to the fermenter, and observing the decrease in dissolved oxygen (DO) concentration (due to cellular respiration) over time with the help of a DO probe. DO levels were not allowed to drop below the 10% critical limit suggested in the literature. The slope of linear regression of the change in DO concentration vs. time for the decreasing curve yielded the OUR, and further dividing the OUR by cell mass concentration gave the specific volumetric OUR. During the OUR measurements constant biomass was assumed based on the biomass trends verified during fermentation experiments. In the second stage, aeration was started again to measure the rate of increase in DO concentrations until a steady oxygen concentration was reached giving oxygen transfer rates. Finally, K_La values were computed as described by Garchia-Ochoa et al. (2000).

Determination of Energy Consumption

Energy consumption by the fermenter, microbubble generator, and delivery pumps was monitored using a Veris H8036 Power Logic Energy Meter operated using Enercept Metering software Version 1.12 (Veris Industries). Results from the energy meter were expressed as net KWH for an entire fermentation run.

Biocompatibility Experiments

Biocompatibility of Tween-20 with *X. Campestris* was verified through shake flask experiments. Four Erlenmeyer flasks were each filled with 100 ml of shake flask medium freshly prepared, and surfactant was added at levels of 0, 120, 300, and 500 ppm. All the flasks were autoclaved at 121^{0}C for 15 minutes and allowed to cool. Two loops of stock culture were transferred from the slants into a tissue culture bottle with 25 ml of sterilized shake flask medium. This culture was then incubated at 28^{0}C for 24 hours, after which 5 ml of inoculum was introduced into the shake flask medium with different surfactant levels. These flasks were kept under incubation at 28^{0}C for 48 hours. Samples were taken at intervals of every 4 hours for OD_{565} measurement on a spectrophotometer to obtain the cell concentration. OD values were later correlated with the standard curve of cell concentration and OD to calculate biomass concentration. Profiles for all samples over time were plotted to observe the effect of surfactant on the microorganisms.

Standardization of Microbubble Generator Process Parameters

Microbubble Property Study

One-liter Tween-20 surfactant solutions at concentrations of 120, 300 and 500 ppm were prepared in 4-L flasks for our experiments. The surfactant solutions were poured into the microbubble generator and treatments given for treatment times of 2, 3, 4, and 5 minutes and processing speeds of 5000, 6000, 7000, and 8000 rpm. Microbubble gas hold-up was calculated at the end of each

treatment by noting the levels of initial and final volume of surfactant solution in the microbubble generator. The microbubble generator was pre-indexed with a standard scale to obtain the information on heights of dispersion in the generator. Stability was assessed by noting the time for separation of microbubbles from the solution. A stopwatch was used to monitor the treatment time and stability of dispersion.

Shear Resistance of Microorganisms

About 1L of fermentation broth from the fermenter at the end of 30 hours of fermentation from a 6-L fermentation run was taken aseptically into a sterilized 4-L flask to study the effect of shear on microbial plate counts. The broth was transferred into a clean and sterile microbubble generator and sheared at 8000 rpm over time. Samples were collected at intervals of 0, 3, 6, 9, and 12 minutes and plated on agar for SPC and counts plotted over time.

Shear Effect on Xanthan Quality

Xanthan quality expressed in terms of molecular weight was studied to assess the effect of shear on xanthan gum in a microbubble generator. Xanthan solutions were prepared separately by dissolving approximately 0.5 and 1% levels in deionized water and solutions taken individually into the microbubble generator. Under standardized conditions for the microbubble generator, solutions were treated and samples taken at intervals of 0, 5, 10, 15, & 30

minutes for molecular weight analysis. Samples were diluted to levels of 0.01% using deionized water before running them on HPLC.

Fermentation Runs

Bench-Scale Fermenter

Fermentation runs were conducted in a 14-L Module MF-114 New Brunswick Microferm fermenter (New Brunswick Scientific Co. Inc., NJ) with built-in pH, air flow, dissolved oxygen (DO), temperature, foam, agitation, and aeration controls. The fermentation was carried out in a detachable stirred Pyrex glass fermenter that could be autoclaved for each experiment. The glass fermenter had the following specifications: vessel diameter-8.5", height-17.5", impeller type-turbine impeller, and number of impellers-1. This glass jar rested on a head plate designed with agitator, heat exchanger and connections for air inlet, air exhaust, inoculation, temperature, pH, air, and many other controls.

The pH measurement was done by Type 465 Metler Toledo pH glass electrode (Cole-Palmer Instrument Co.) connected to an Auto pH controller, Model pH-40 (New Brunteswik Scientific Co., Inc. NJ). A 115 V / 4 amp output from the pH controller operated 2 variable-speed peristaltic pumps (Masterflex C/L PUMP SYSTEM, Model #77120-20, Cole Palmer Instrument Co. IL) regulating automatic addition of 5M (molar) NaOH into the fermenter in order to maintain the desired pH value. Air sparging was done through a removable single-orifice sparger, and flow rate was controlled by an air flow meter with operating range of 1,600-16,000cc/min. In order to supply sterile air to the fermenter, the air from the compressor was directed through a 0.2-micron

membrane filter before passing it through the sparger. Dissolved oxygen (DO) was measured using polarographic Ingold probes connected to a DO-81 controller (New Brunswick Scientific Co. Inc., NJ) equipped with chart and printer for DO profiling during the fermentation run. Temperature in the fermenter was measured by a resistance temperature detector (RTD) and controlled with a thermostat by automatic circulation of hot or cold water from the cold-water inlet to the fermenter passing through a cartridge type immersion stainless steel heater. The agitation unit was designed for an operating range of 100-1,000 rpm. Agitation, foam, and aeration controls, although part of the system, were not used for the fermentation conditions studied.

Preliminary Experiments

Preliminary experiments were conducted to profile the DO patterns during 6-L fermentation runs operated at conditions of 0.2 vvm air flow rate; agitation speed of 300 step 600 rpm; DO levels of >10% through out the experiments; pH 7 and Temperature of 28^{0}C. Similarly, fed-batch runs were conducted with 4L initial volume and 2L supplement at the point of DO drop to 20% in the fermenter to profile the DO patterns at operating conditions as mentioned above.

Fermentation Runs with Air Sparging

Before every run, the fermentation lab was cleaned and steam-sterilized in order to ensure sterile conditions. Personal hygiene considerations were also ensured during fermentation experiments. The fermentation medium containing

glucose and minerals was weighed appropriately on a calibrated weighing balance and dissolved in deionized water in large 6-L conical flasks, sterilized separately in an autoclave at 115^0C for 15 minutes followed by cooling before transferring it to a sterile fermenter. The fermenter assembly was sterilized in an autoclave at 115^0C for 15 minutes and allowed to cool. The DO probe was first soaked in boiling water for ~ 1 hour to remove the gas bubbles from the sensors tip followed by polarization for not less than 12 hours by keeping the DO membrane tip soaked in polarographic filling solution [60% glycerol, 7.45% KCL, 32.55% water] before use in the fermenter. It was then alcohol-sterilized and inserted into the DO port on the fermenter assembly. The pH probe, connected to an auto pH controller, was calibrated using pH 4 & 7 buffer (VWR Scientific products, PA) before each experiment, and the pH controller was held in the stand-by mode. It was then alcohol sterilized and inserted into the pH port of the fermenter assembly. Next the fermenter glass jar was filled with the medium through the inoculum port under warm conditions and the fermenter assembly was fit into the fermenter armature. Water inlet and exit lines, connectors for the drive and agitator, air inlet and exit, temperature controller, pH, and DO controller connections were then made to the fermenter.

The fermenter was turned ON and the agitator set to 300 rpm, with water supply lines opened. This facilitated cooling and mixing of media to set the temperature to 28^0C. Once temperature was reached, the pH controller was turned to the "measure mode", enabling pH adjustment to 7 by pumping of base into the fermenter. Next DO probe calibration was performed by starting on the

DO controller and replacing the air supply with nitrogen into the medium, allowing the DO to drop to 0% oxygen tension. The DO controller was calibrated to zero using the "Zero adjustment" provided on the controller. Then, the nitrogen supply was stopped, and the air supply to the fermenter was resumed to allow the DO level to increase to 100% oxygen tension. The DO controller was then calibrated to 100 by setting the "span adjustment", completing the DO probe calibration. In order to monitor the power consumption by the fermenter, the energy supply inlet to the fermenter was plugged into the port connected to the power logic energy meter and set to "zero". This completed the initial preparation procedures for the fermenter.

The inoculum prepared by incubation for 24 hours at 28^0C as described in the inoculum preparation procedure was now added to the fermenter at 3.33% through the inoculum port. Fermentation was then allowed to proceed for 60 hours. Samples were taken at intervals of 6 hours from the sample port and kept in the refrigerator at 4^0C for further analysis. Fermenter volume was operated at 6 L initially for 6-L experiments and for fed batch experiments, glucose was added in a fed-batch mode, with 40g/L added initially, followed by an additional 10g/L toward the end of the exponential growth phase of cells. Agitation speed was set to 300 rpm (until first DO drop) then stepped up to 600 rpm. The pH was controlled at 7.0 by not allowing acidic conditions to prevail in the fermenter, but for pH increases above 7, no control was ensured. Airflow rate was set to 1,200 cc/min, and this rate was selected taking into consideration microbubble delivery capacities possible for our experiments. Temperature was held constant at 28^0C

throughout the experiments. A DO level above 10% was ensured throughout the experiments to avoid negative effects on product formation. The experimental set-up with controls for this study is shown in Figure 7.

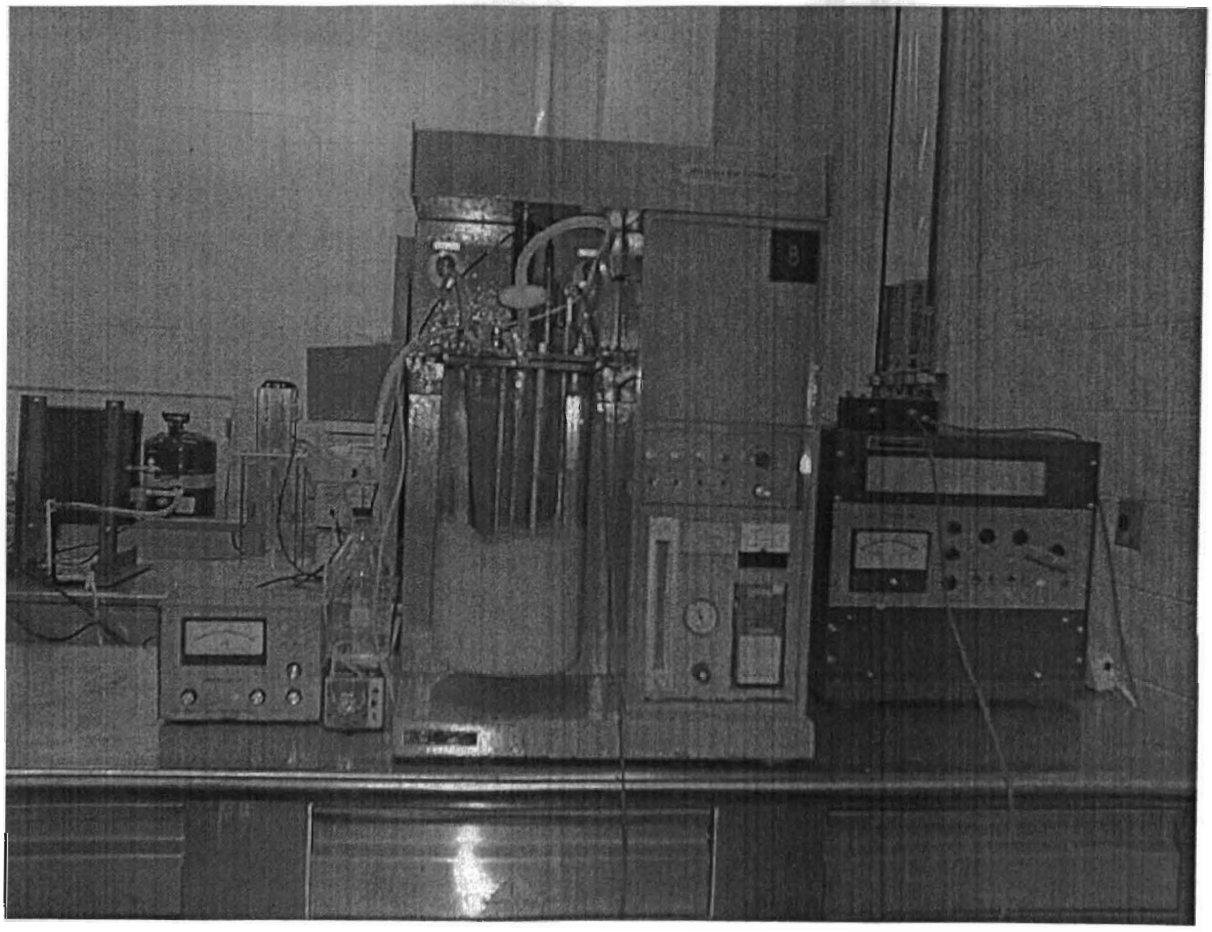

Figure 7. Experimental set-up used in fermentation experiments involving air sparging

Fermentation Runs with Microbubble Sparging

With the rest of the conditions remaining the same as explained in air sparging, microbubble sparging involved delivery of microbubbles from the microbubble generator operated under standardized conditions based on microbubble generator experiments. The microbubble generator was cleaned with hot water, sterilized with alcohol, and allowed to dry before each experiment. The Masterflex hose tubing (24" Neoprene), air inlet line, and other accessories used to connect the fermenter and microbubble generator were sterilized in an autoclave under conditions similar to those mentioned above.

At the peak exponential phase of microorganism growth (derived from preliminary experiments), fermentation broth was circulated by a Masterflex peristaltic pump through the microbubble generator operated under standardized conditions for 30 minutes at intervals of 6 hours untill the end of the fermentation run. OUR and OTR measurements were made at the end of the microbubble delivery to gather information regarding mass transfer and to make comparisons with air sparging. In the case of the 4+2 L fed-batch fermentation runs, 2 L of fed batch media was used directly in the microbubble generator and microbubbles delivered to the fermenter. Throughout the process of microbubble delivery, a microbubble dispersion flow rate of 600 ml/min or equivalent air flow rate of ~360 ml/min was set. During this process airflow to the fermenter was shut down, and air inlet flow to the microbubble generator was set at 1,200 cc/min. The inlet flow of fermentation broth to the microbubble generator was regulated manually to achieve the desired standardized conditions obtained through microbubble

generator experiments. The experimental set-up with the fermenter connected to the microbubble generator is shown in Figure 8.

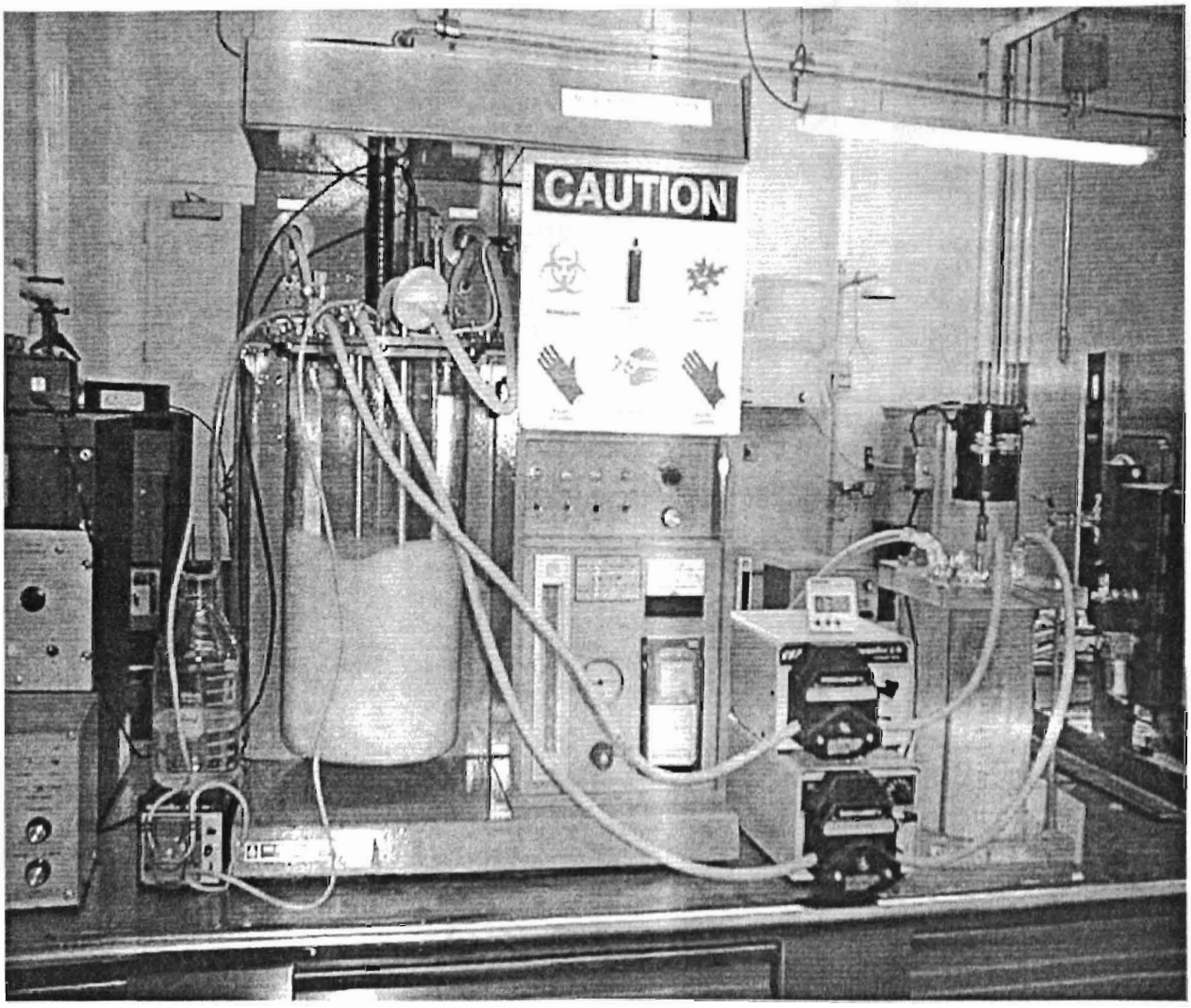

Figure 8. Experimental set-up used in fermentation experiments involving microbubble sparging

CHAPTER IV
RESULTS AND DISCUSSION

This chapter contains the results obtained for experiments on Tween-20 biocompatibility with *X.campestris*, the effect of microbubble parameters on microbubble quality, and the effect of shear within the microbubble generator on microorganisms and xanthan quality. In addition, results are shown for fermentation runs comparing the partially substituted microbubble sparging with ordinary air sparging based on biomass growth, xanthan production, pH, oxygen uptake rate, volumetric mass transfer coefficient and final xanthan quality profiles.

Biocompatibility of Tween-20 with *X. campestris*

The effect of the surfactant Tween-20 at different concentrations on *X. campestris* organisms was studied in order to determine whether the organism is compatible with the surfactant. Shake flask experiments were conducted to study biomass growth in the presence of various concentrations of surfactant. Figure 9 shows a comparison of biomass profiles with time for different surfactant levels and a control. Results indicate that surfactant Tween-20 had no effect on the biomass growth profiles of *X. campestris* organisms for surfactant levels up to 500 ppm. The cell densities after 80 hours of growth ranged from 2.9-3.1g/litre for surfactant levels of 0-500 ppm indicating that surfactants had no inhibitory effect on the cell growth. This conclusion is supported by Table 1, which shows the

effect of surfactant concentration on specific growth rates of *X.campestris* organisms. In the table, surfactant levels are expressed as dimensionless surfactant concentration (DSC, which is the ratio of surfactant concentration to its critical micelle concentration (120 mg/l)). From the table it can be seen that Tween-20 showed no negative effect on specific growth rates. Rather, surfactant increased cell growth, as an increase in DSC resulted in an increase in specific growth rates. Specifically, an increase in DSC from 0 to 4.17 resulted in an increase in specific growth from 0.0619 to 0.0684. Similar results indicating non-toxicity of Tween-20 towards culture systems like soy and carrot suspension cultures, *B. methylotrophicum* (Bredwell et al., 1997) and further enhancement of cell growth in *B. methylotrophicum* have been reported. The nontoxic nature of Tween-20 has been attributed to its longer chain length, hence causing slower diffusion into the cell membrane.

Table 1. Specific growth rate (hr^{-1}) for *X.campestris* in the presence of different surfactant concentrations

Concentration of Tween-20 in ppm	**DSC for Tween-20**	**Specific growth rate (hr^{-1})**
0	0	0.0619
120	1	0.0636
300	2.5	0.0665
500	4.17	0.0684

* DSC = Dimensionless surfactant concentration

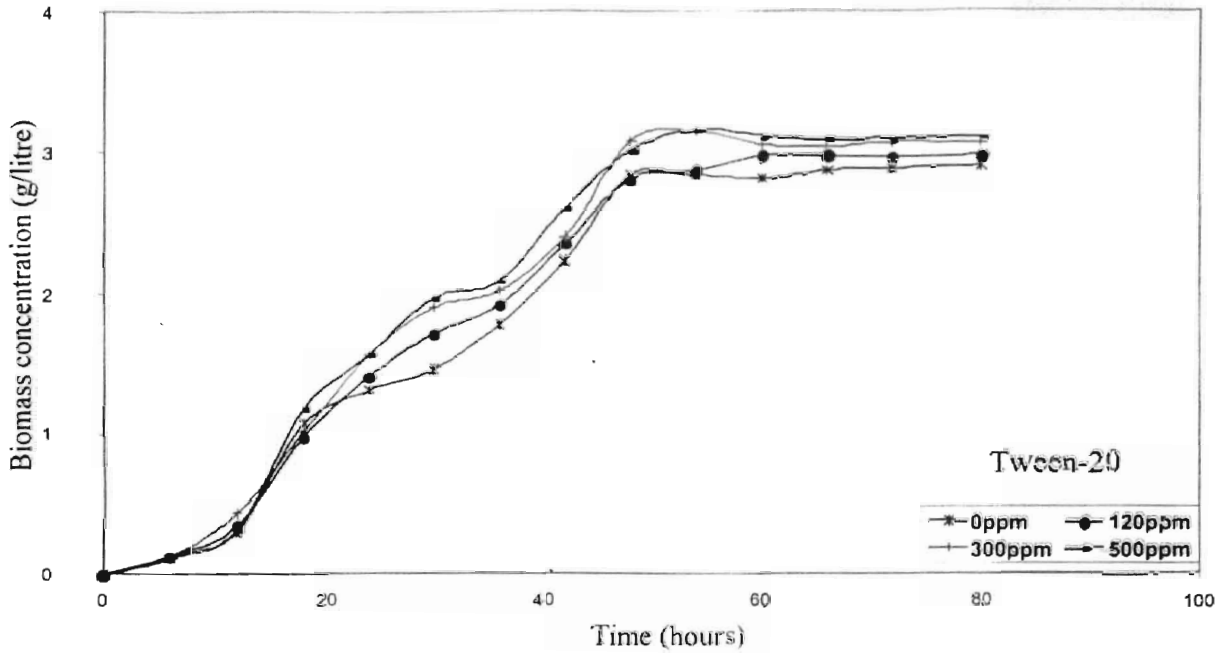

Figure 9. Biomass growth in the presence of various levels of Tween-20 vs. time

Microbubble generation

Effect of Process Variables on Microbubble Properties

For initial testing, water was used as the media. The study of microbubble properties in the microbubble generator involved varying process parameters such as agitation speed, processing time, and surfactant concentration to determine their effect on gas hold-up and foam stability. Figure 10 shows the results of process parameters on gas hold-up. Figure 11 shows the results of process parameters on foam stability. From the figures it can be seen that with increasing agitation speed, an increase in air content and foam stability was observed. Higher degree of stability at higher gas hold-up could be explained by

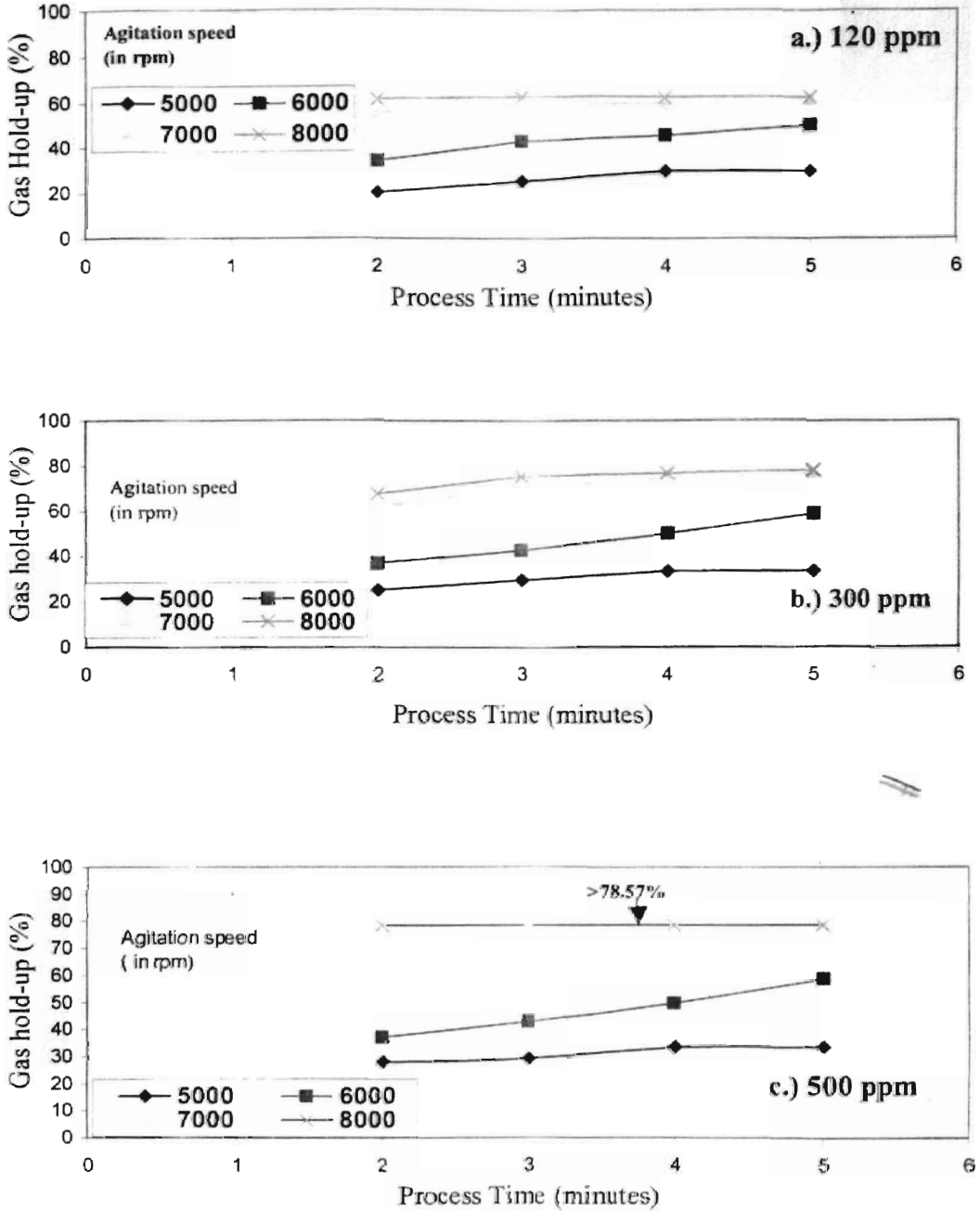

Figure 10. Effect of agitation speed and process time in microbubble generator on gas hold-up at Tween-20 levels of a.) 120 ppm, b.) 300 ppm, and c.) 500 ppm

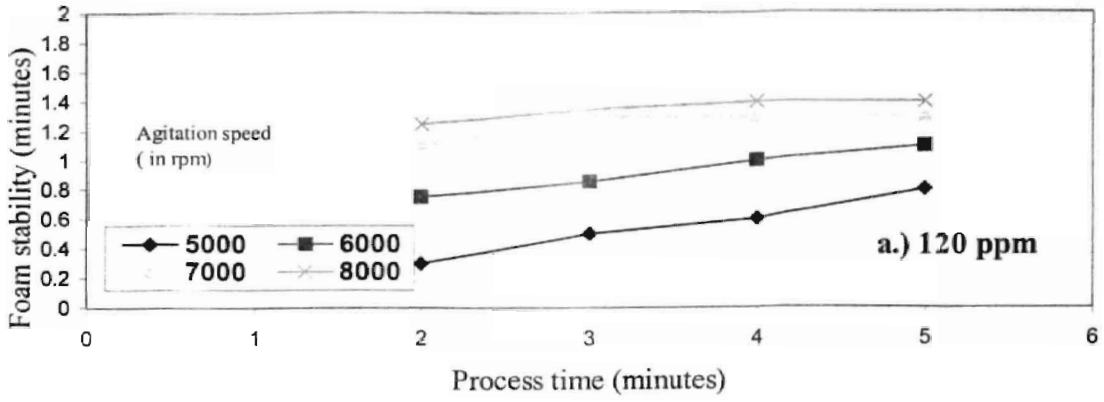

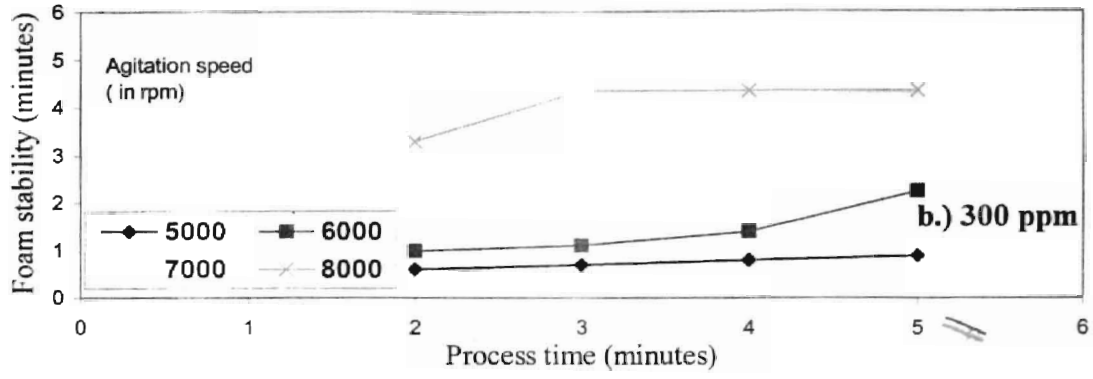

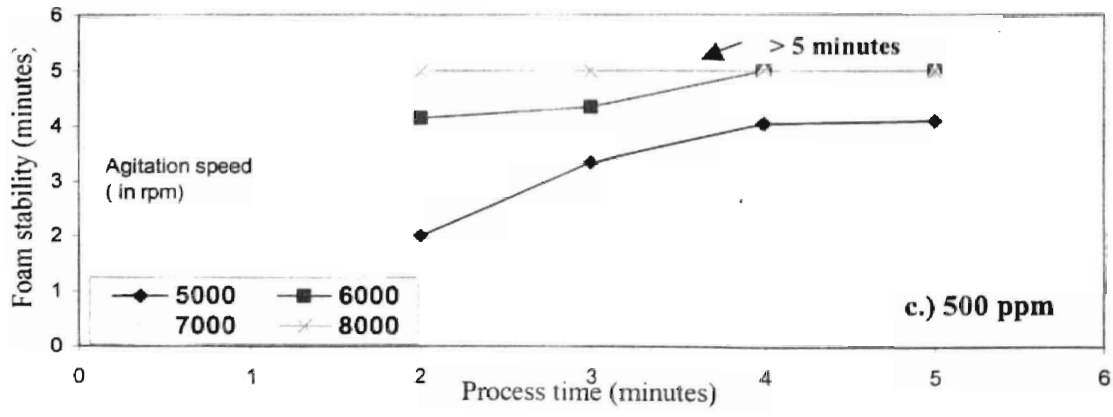

Figure 11. Effect of agitation speed and process time in microbubble generator on foam stability at Tween-20 levels of a.) 120 ppm, b.) 300 ppm, and c.) 500 ppm

the fact that smaller bubbles contributed to greater stability. Matsushita et al. (1992) reported a larger increase in air content and air stability with an increase in agitation speed from 5,000-5,500 rpm and a slight increase in air content and stability with an increase in agitation speed from 5,500-8,500 rpm. An increase in process time increased air content and foam stability slightly, which could be explained by the fact that a longer duration of treatment enables increased air entrainment and also formation of smaller bubbles due to longer shearing time. Matsushita *et al.* (1992) and Jauregi *et al.* (1997) reported that an increase in stirring time from 0.5 to 5 minutes slightly increased the air content for CTMAB (cetyltrimethyl ammonium bromide) surfactants. However, Matsushita *et al.* (1992) reported no effect on stability with increase in processing time. This difference in results regarding stability may be due to differences in the nature of the two surfactants.

An increase in surfactant levels increased gas hold-up, and the increase was more significant at high agitation speeds of 7,000-8,000 rpm than at lower agitation speeds. The result could be due to the fact that higher agitation speeds are necessary to see the effect of increased surfactant levels on air content. Chapalkar *et al.* (1993) also reported higher gas hold up values with increasing surfactant concentrations. Matsushita et al. (1992) reported that an increase in surfactant levels from 0.25 to 2.5 g/l had a great influence on stability, but not on the air content values when CTMAB surfactant was used in the study. Higher surfactant levels increased the stability, and the increase in stability values was larger for surfactant concentrations between 300 and 500 ppm than between 120

and 300 ppm. At 300 ppm and agitation speeds of 7,000-8,000 rpm, gas hold-up values ranged from 62-78% and stability values from 3-4.35 minutes. However, at a surfactant concentration of 500 ppm and agitation speeds between 7,000-8,000 rpm very high air content values above 78% and foam stability of ~5 minutes were attained. This explains the effect of surfactant in formation of microbubbles that are smaller, yet more stable, which could possibly be due to formation of a stable film around the air bubbles.

Based on our requirements on the fermentation operating conditions (air flow rate, agitation speed, fermentation volume) and the previous information on microbubble properties, an agitation speed of 8,000 rpm, surfactant level of 300 ppm, and 2 minutes process time were selected as optimum for looping the microbubble generator with fermenter. As can be seen from the figures 10 & 11, at these microbubble generator conditions, microbubbles generated have a gas hold-up of 68% and stability values of 3.3 minutes, which are well above our assumed requirements for microbubble quality (gas hold-up ~ 65% (Matsushita et al., 1992) and stability ~3 minutes (hypothesized from the time lag between generation through delivery and desired residence time in fermenter).

Effect of Media on Microbubble Properties

Once these operating conditions were optimized with water, the microbubble properties for water were compared to those of media containing 0, 0.5 and 1% xanthan levels so as to simulate the conditions in the fermenter during actual fermentation. The results of this study are presented in Table 2. It was observed that gas hold-up decreased with increasing concentration of

xanthan in the media in comparison to water. The decrease in air content could be explained by inadequate mixing with a single spinning disc in the microbubble generator due to an increase in viscosity of the medium. Microbubble stability trends were quite the opposite, as an increase in stability values was observed. For all the conditions studied, stability values were > 3 minutes. This increase in stability values could be attributed to the increase in viscosity of medium that could be preventing the formed microbubbles from expanding in size, thereby resulting in increased stability.

Table 2. Effect of media on microbubble properties

Microbubble properties	Water	Media	0.5% xanthan	1% xanthan
Gas-hold-up (%)	68	65.3	59.6	56
Foam stability (minutes)	3	>3	>3	>3
Interfacial area (%/micron)	10.68	8.27	5.32	2.6

As measured by a laser particle size analyzer, the average microbubble size (Figure. 12) for standardized conditions in water was about 120 μ, similar to the results of Bredwell et al., 1995. However, in media, the size increased to 140 μ, which could be due to the effect of minerals and other media constituents and also due to high sugar concentrations in the media, leading to an increase in viscosity and hence an increase in size. Further increase in xanthan

concentration from 0 to 1% caused increase in average particle size from 140 μ to 400 μ, and the size increased with increase in xanthan concentration in media. It was also observed that the microbubble distribution shifted from a monomodal to a bimodal distribution, which explains the observed presence of a dispersion of larger and smaller bubbles in the microbubble generator. However, with the use of multiple spinning discs in the microbubble generator, lower particle sizes could be achieved. Using the average microbubble diameters, the interfacial areas were calculated. Interfacial areas available with the microbubbles for the different media ranged from 2.6-10.08 %/micron in comparison to ordinary air sparging (average bubble size assumed-3.5 mm), which was 0.17 %/micron. This increase in interfacial area shows the potential importance of microbubbles in enhancing mass transfer in xanthan fermentation.

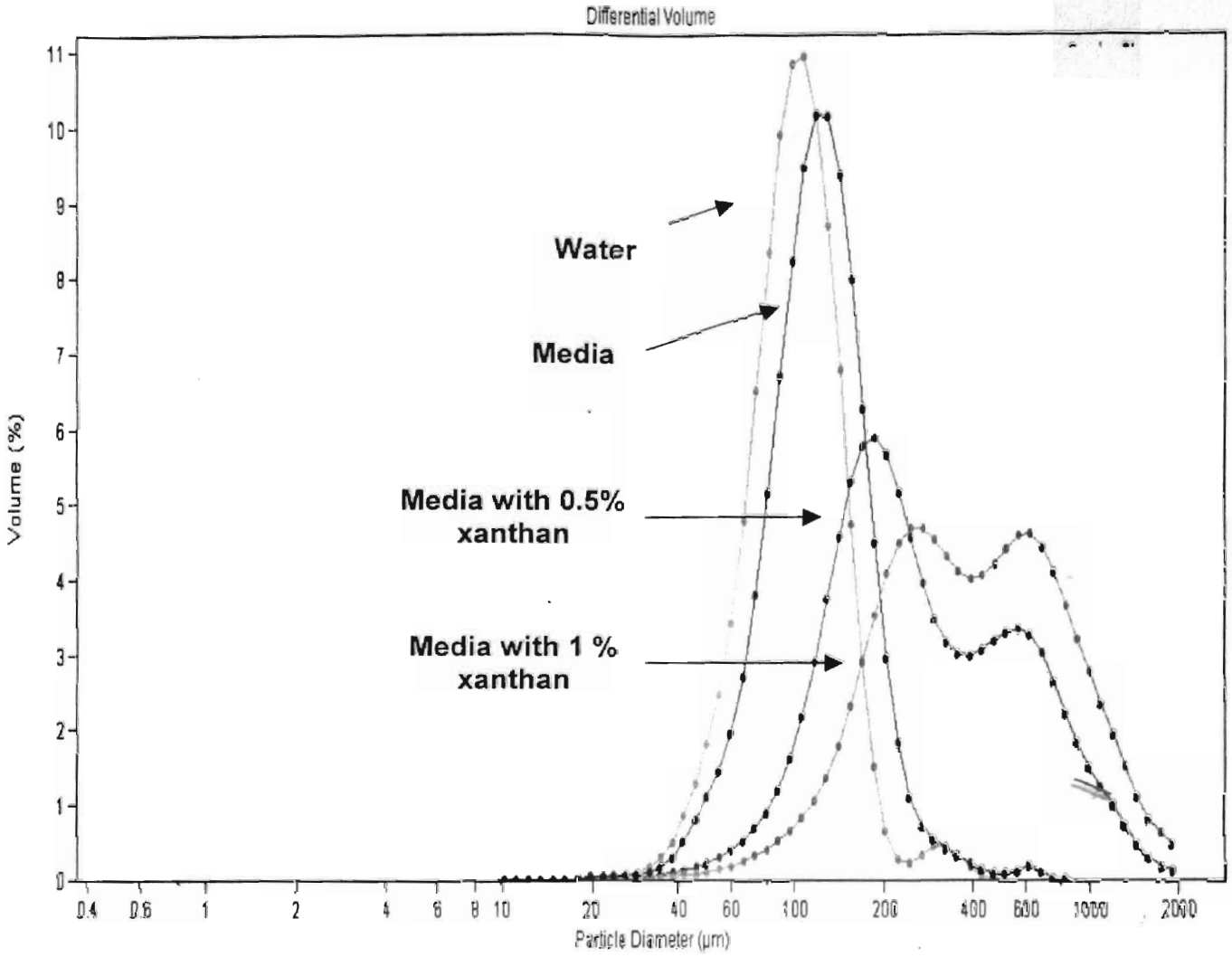

Figure 12. Microbubble size distribution on a Laser particle size analyzer for media with different xanthan levels (media was exposed to 8000 rpm in the microbubble generator with 300ppm Tween-20 for 2 minutes)

Effect of Shear Force on *X. Campestris* Organisms

In order to determine the viability of the *X.Campestris* organisms in the microbubble generator, shear experiments on the organism were conducted for the optimized operating conditions of the microbubble generator. Results are expressed as standard plate count vs. time in Figure 13. It was observed that

upon continuous shear of the same media containing cells, counts decreased slowly with time, yet at very low rates, indicating the shear resistant nature of these organisms in the microbubble generator. It can be seen from Figure 13 that cell counts decrease by ~32%. This situation was a bit extreme, in that cells in the same medium (~0.2% xanthan) were being continuously sheared for about 12 minutes. However, in actual experiments the medium would be circulated from the fermenter through the microbubble generator, and the residence time would be ~2 minutes, with xanthan levels beyond 0.5%. With increasing xanthan levels during fermentation, it is hypothesized that cells would show considerable resistance to shear, because the gum around the cell could protect the cells while in the microbubble generator.

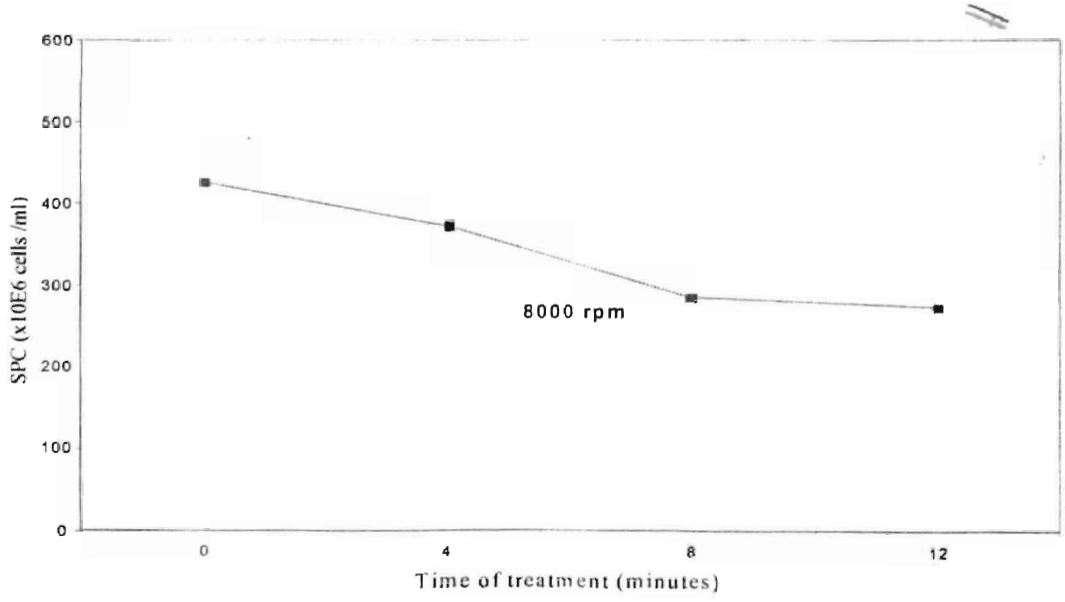

Note: Results are average of duplicate runs

Figure 13. Effect of shear in the microbubble generator on X.Campestris

Effect of Shear in Microbubble Generator on Xanthan Quality

In order to verify whether shearing conditions within the microbubble generator will have any effect on xanthan quality, the effect of shear on molecular weight distribution of xanthan was studied and obtained results for each condition from HPLC analysis. The effect of shear on molecular weight should result in changes in HPLC retention time, base line (start and end), peak height & width, and area if xanthan molecular weight is affected. Figures 14 and 15 show the various HPLC indices with time for 0.5% and 1% xanthan solutions respectively. The fact that all of the curves were flat with time indicates that there was no significant effect on xanthan quality even after continuous shearing of the solution for a duration of up to 30 minutes. Further, since normal microbubble operation will involve circulating the broth from the fermenter into the microbubble generator, with relatively short residence times of ~ 2 minutes, it is hypothesized that the shear encountered in the microbubble generator will not have any effect on the xanthan quality.

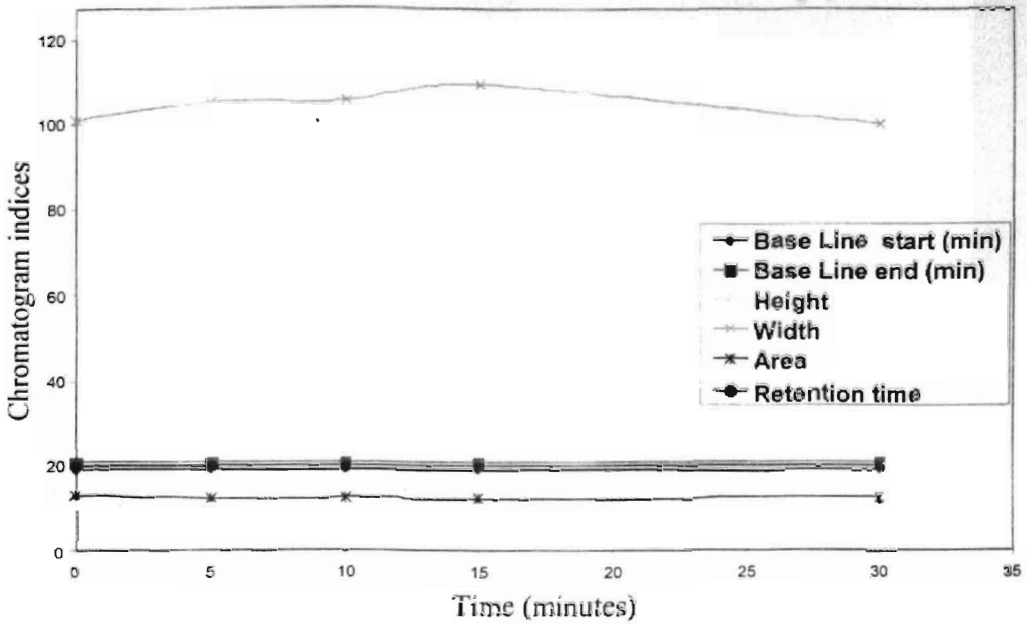

Figure 14. HPLC indices for 0.5% xanthan solutions in Microbubble generator

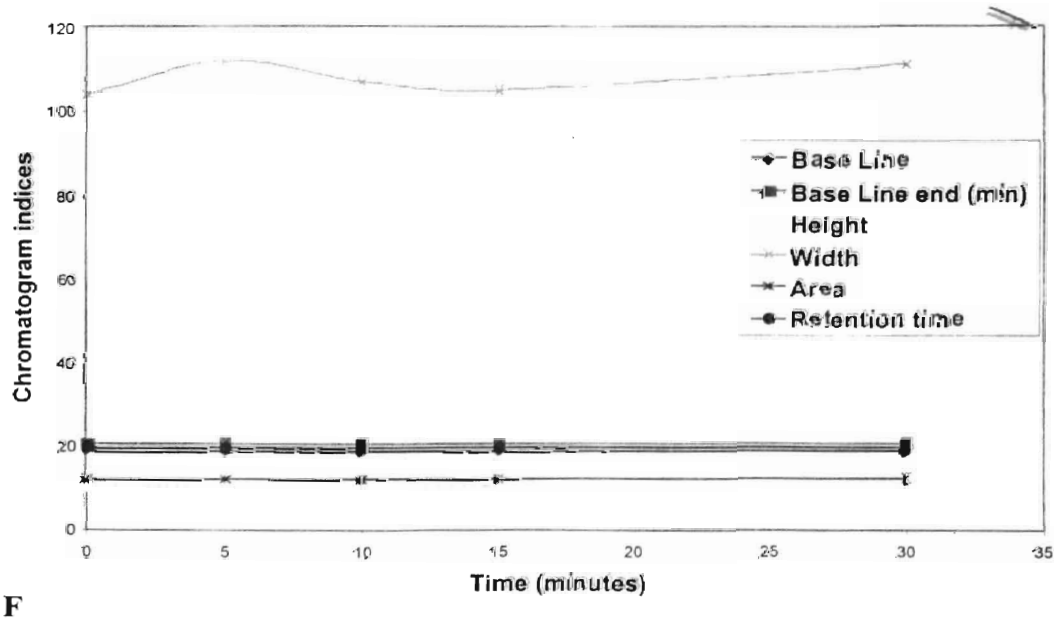

F

Figure 15. HPLC indices for 1% xanthan solutions in Microbubble generator

Fermentation Runs

Preliminary Experiments

Preliminary runs were conducted to profile the dissolved oxygen (DO) patterns in the fermenters during 6L and 4+2L fed batch fermentation experiments. Figure 16 shows the DO profiles for 6L and 4+2L fed batch fermentation experiments. From the figure, it can be seen that the DO remained steady in both the fermenters initially, after which it appeared to drop steadily and then reached levels of 20% at the 18^{th} hour for fed batch runs in comparison to the 21^{st} hour for 6L fermentation runs at agitation speed of 300 rpm. The drop in DO represents the point of maximum cell concentration in the fermenter, and hence the increased uptake of oxygen. In order to ensure that DO levels remain above 20% through out the fermentation, it is at this point that agitation speed is increased to 600 rpm. Immediately following the increase in agitation, a rise in DO levels occurs, after which it remains fairly steady.

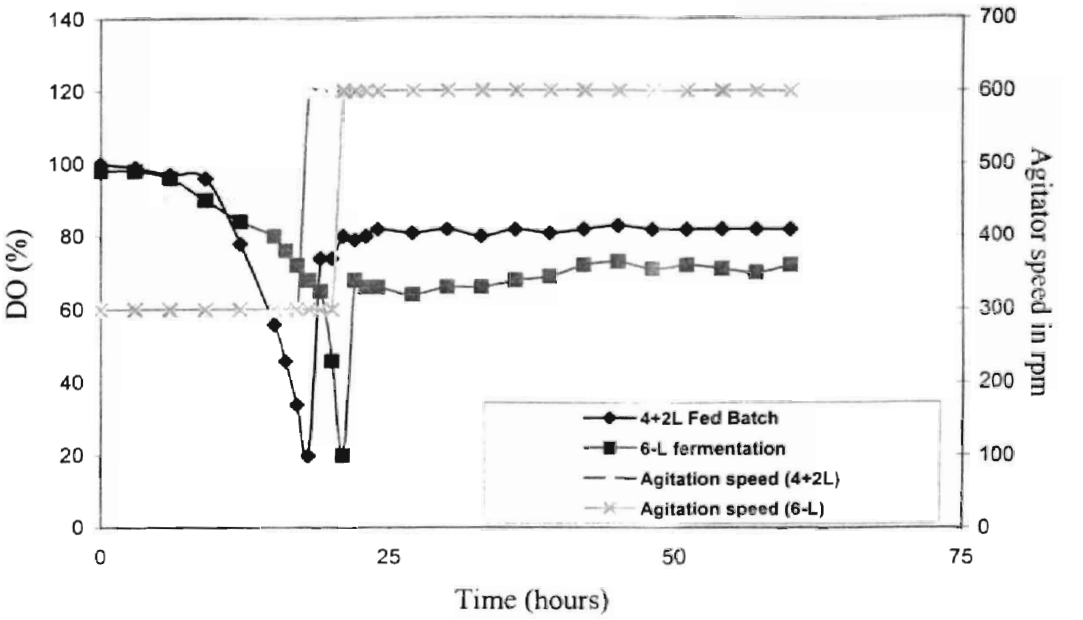

Figure 16. Dissolved oxygen trends for 6-L and fed-batch experiments

Effect of Microbubbles on Dissolved Oxygen Profiles

Figures 17 and 18 show the DO comparisons for air and partially substituted microbubble sparging in both 6-L and 4+2L fed-batch fermentation experiments. The trends indicate that an agitation speed of 300 rpm was maintained for the first 18 hours (4+2L fed-batch) and 21 hours (6-L runs) followed by a step-up to 600 rpm until the completion of the run. Comparisons of DO profiles with both approaches shows that the DO level remained steady initially followed by a sudden drop after the 16th hour (4+2L fed-batch) and 18th hour (6-L runs) until it reached 20% at 18th and 21st hour respectively. By stepping up the agitation speed again to 600 rpm the DO levels increased to ~60% and remained above 60% until the end of the fermentation run when it reached levels of ~ 70% for both approaches. Almost similar trends were noticed

in partially substituted microbubble sparging runs except that with the introduction of microbubbles there occurred a simultaneous drop in DO level, and this trend remained through out the experiment (both 6-L and 4+2L fed-batch) when microbubbles were introduced. An "enlarged image" of the DO drop in the microbubble sparging runs is shown in Appendix. A.15.Two possible explanation for the drop in DO level are the differences in flow rates between air and microbubble sparging (microbubble sparging had a dispersion flow rate of half that of air sparging) and possibly due to better oxygen utilization in the fermenter.

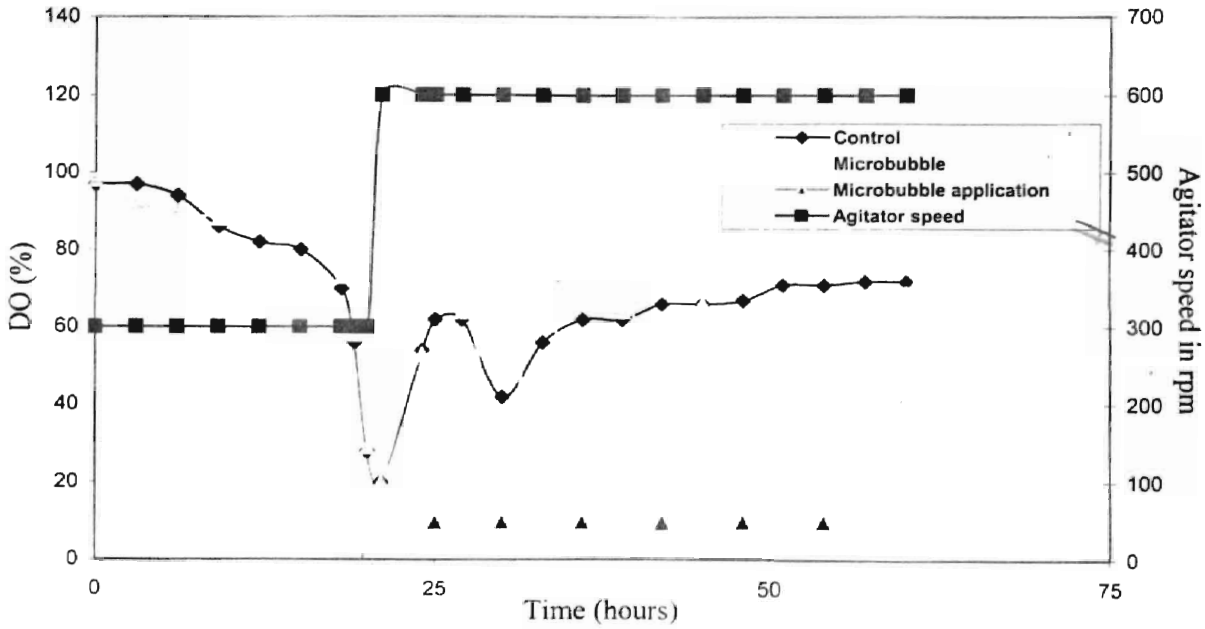

Figure 17. Dissolved oxygen comparisons with time for air and partially substituted microbubble sparging fermentations

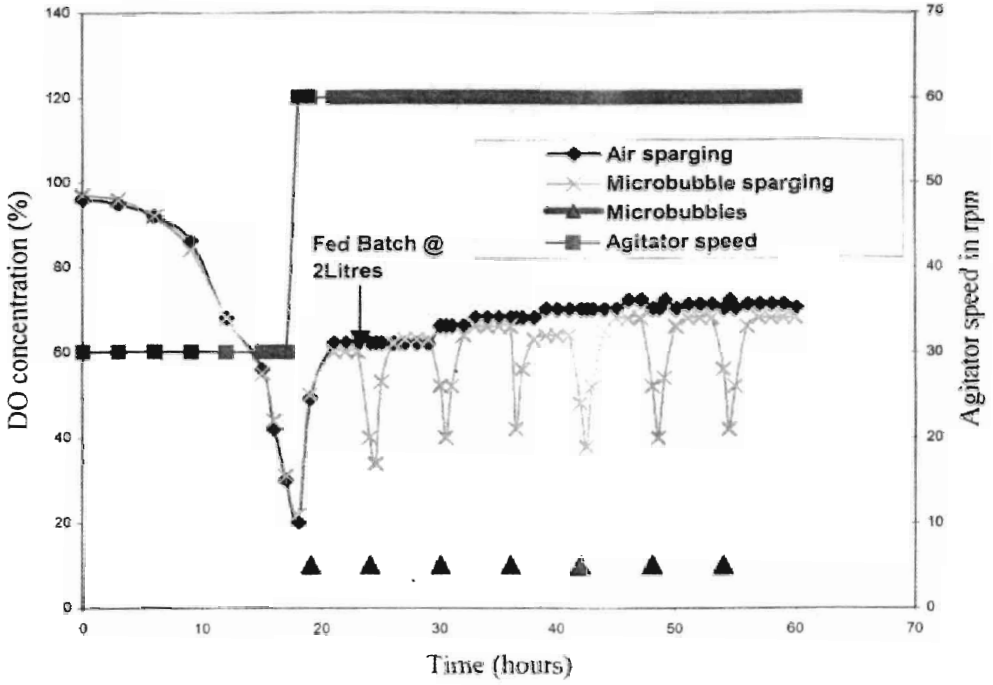

Figure 18. Dissolved oxygen comparisons with time for air and partially substituted microbubble sparging Fed-batch experiments

Effect of Microbubbles on pH Profiles

Figure 19 shows the pH profile with time during the fermentation runs with both approaches. It can be seen that pH remained at 7 for the first 24 hours since the lower limit of pH was controlled at 7 by the addition of 5M NaOH. However, after 24 hours the pH shifted towards alkaline conditions and the rate of shift was higher in the fermenter with partially substituted microbubble sparging in comparison to air sparging. The final pH at the end of one of the 6L runs was 8.3 and 7.9 respectively for both the microbubble and air sparging approaches. The increasing pH also serves as an index for increasing activity of microorganisms in

terms of growth and xanthan gum production due to the use of microbubbles resulting in increasing pH during fermentation.

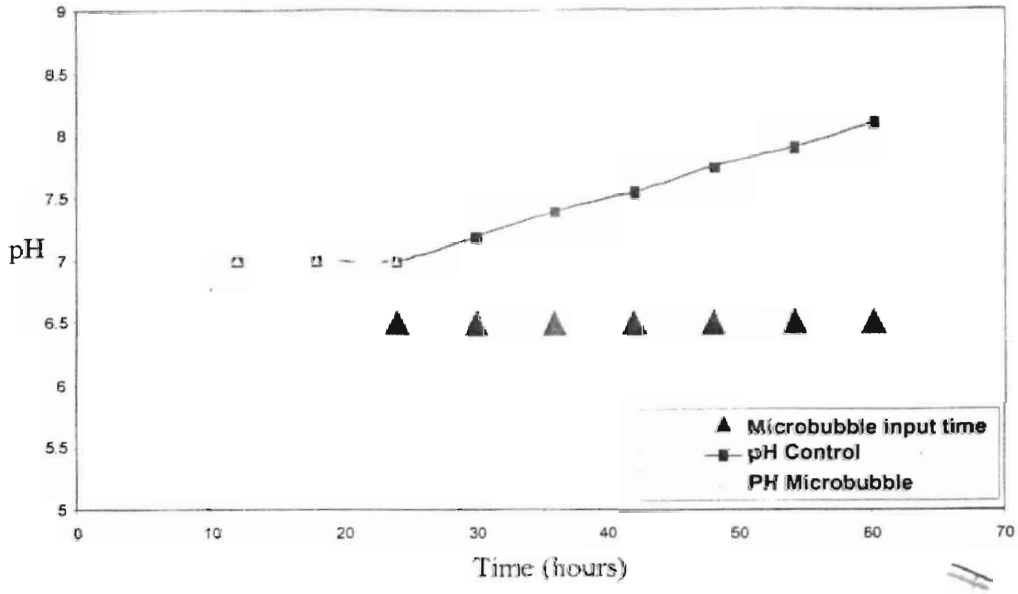

Figure 19. pH comparisons with time for air and partially substituted microbubble sparging fermentations

Effect of Microbubbles on Biomass Profiles

Figure 20 shows biomass concentration profiles for six different fermentation runs: three with air sparging and three with microbubbles compared individually. The initial cell density after inoculation into the fermenter was ~0.05g/l in all the fermentation runs. The comparative profiles of biomass concentration shows that growth trends were very similar in all runs with a short lag phase of ~ 6 hours followed by a log phase that lasted until approximately the

36th hour and then a stationary phase until the 60th hour. With the introduction of microbubbles after 24 hours, an increase in biomass concentration was observed for microbubble sparging in comparison to air sparging and this trend continued until the end of the experiment, yielding a higher final biomass concentration. In each comparative run, final biomass concentrations with microbubble sparging were higher than those involving air sparging alone. In run 1, biomass levels for microbubble and air sparging were 1.88 and 1.76 g/L. Similarly for runs 2 and 3, biomass levels for microbubble and air sparging were 1.97 and 1.69g/L respectively; and 2.29 and 2.09g/L respectively. Further, increased specific growth rate values for microbubble sparging runs were observed in comparison to air sparging (average of 3 runs: $\mu. = 0.72\ h^{-1}$ for microbubble fermentations and $\mu. = 0.66\ h^{-1}$ for air sparging fermentations). This increase in cell concentration (~20% maximum) and specific growth rate values could be attributed to better oxygen utilization by microorganisms with introduction of microbubbles into the fermenter. This could have also contributed to a partial drop in DO in the fermenter when microbubbles were introduced into the

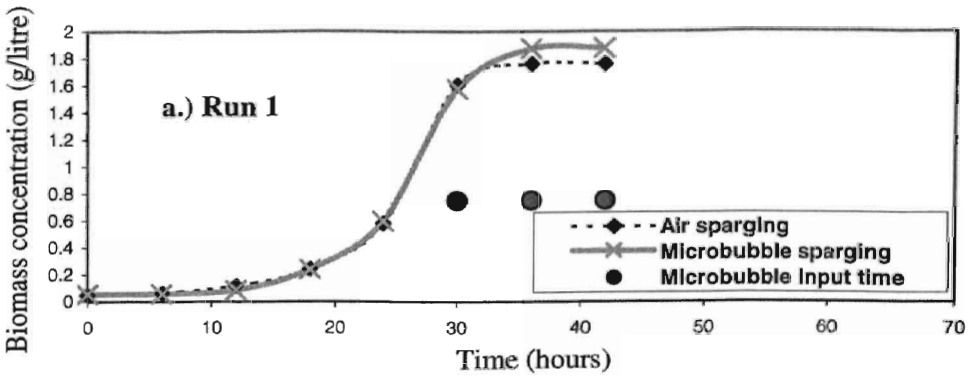

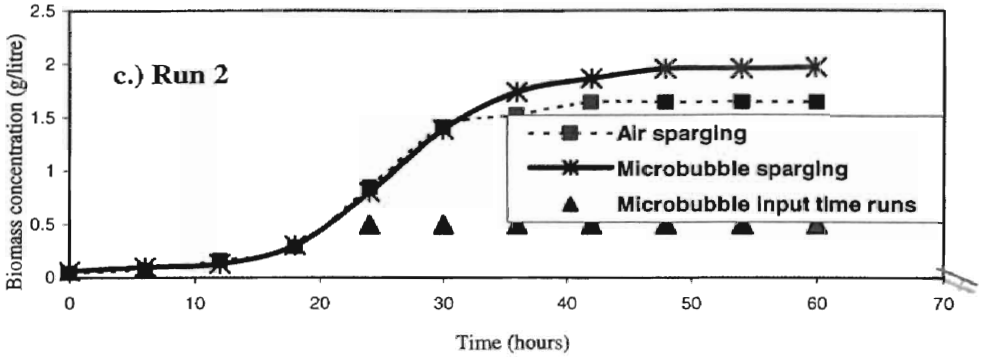

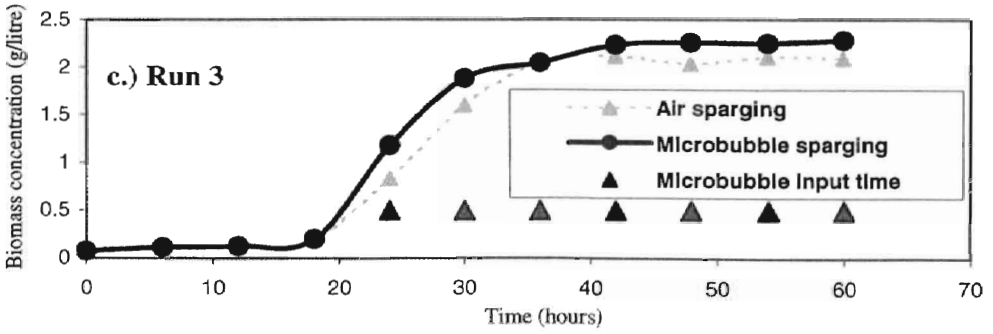

Figure 20. Biomass comparisons with time for air and partially substituted microbubble sparging fermentation experiments (6L) for a.) Run 1, b.) Run 2, and c.) Run 3

fermenter. The results of increase in biomass levels during microbubble sparging are significant in comparison to air sparging due to the fact that the trends between the experiments for air sparging showed no significant variation in biomass trends during biocompatibility experiments.

Early fermentation runs involved fed-batch experiments in order to avoid shearing the entire fermentation broth within the microbubble generator. In the fed-batch runs, initial fermenter volume was 4L, with the additional 2L media being added as microbubbles. Figure 21 shows biomass concentration profiles for the fed-batch experiments and a control. We did not see the effect of fed-batch media delivered in the form of microbubbles at the 20th hour, but we do notice the effect of microbubbles after the 24th hour in terms of biomass growth. The final biomass yields were 1.88 and 1.66g/liter for microbubble and air sparging respectively. The increase in biomass (~13.25%) concentration further confirms the effect of microbubbles in the xanthan gum fermentation. Pramuk (2000) observed similar increases in cell concentration with the introduction of microbubbles and he observed that at low agitation speeds of 150rpm the biomass increased by 1.5 and 1.7 fold in 1L and 50L volume yeast fermentations in comparison to air sparging fermentations. Also Hensirisak (1997) reported increases in biomass concentrations of yeast cells in 1-L and 20-L fermentations with microbubble sparging when compared to air sparging experiments, but no significant effect in biomass levels was observed in 50-L fermentation runs.

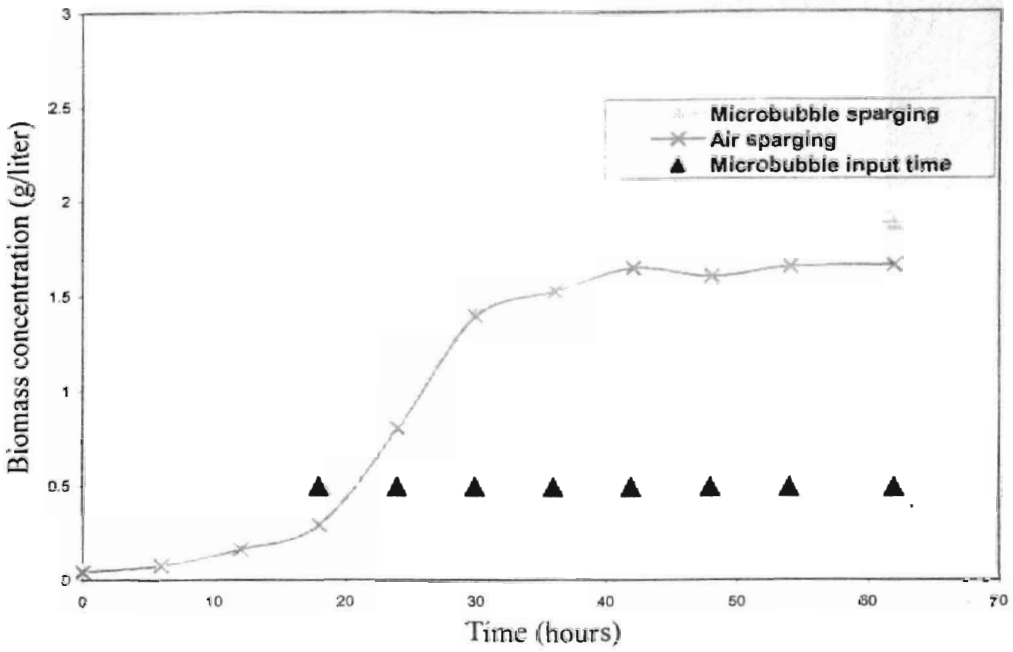

Figure 21. Biomass comparisons with time for air and partially substituted microbubble sparging fed batch fermentation experiment

Effect of Microbubbles on Xanthan Profiles

Figure 22 shows the xanthan gum profiles with time during fermentation runs with microbubble and air sparging. Xanthan concentration remained constant initially for the first 24 hours for both the approaches. However, with the introduction of microbubbles into the fermenter at the 24th hour, xanthan yield increased and continued to show an increase up to the 60th hour, in comparison to air sparging. This increase resulted in final xanthan concentrations for microbubble sparging of 13.24, 15.92 and 12 g/l for the 3 runs, compared to 11.85, 12.14 and 9.52g/l for air sparging. The increase in the xanthan yield (~30%maximum) can be attributed to better oxygen transfer in the fermenter due to microbubbles, enabling increased cell mass accompanied by an increased rate of product formation. The drop in DO, increase in pH and increase in

biomass concentration further support the increase in final product yield with the use of microbubbles.

A similar effect from microbubbles was observed in fed-batch fermentations (Figure 23) where final xanthan yields increased by about 15.3% (from 14.44 to 12.52 g/liter) for microbubble sparging in comparison to air sparging alone.

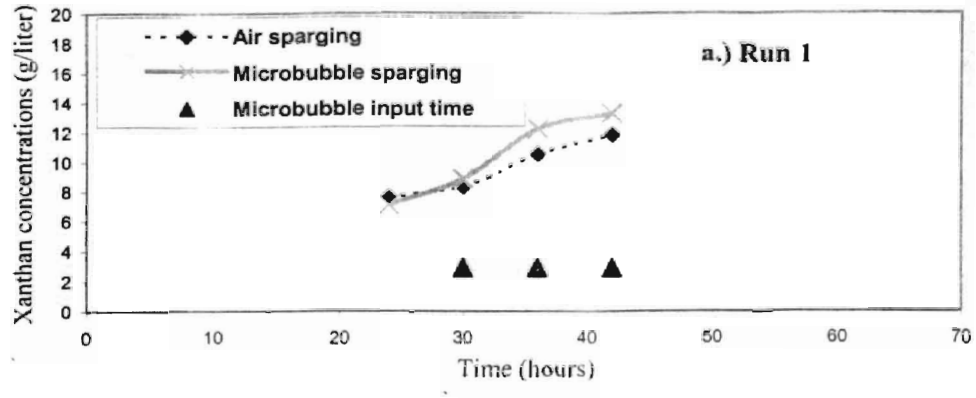

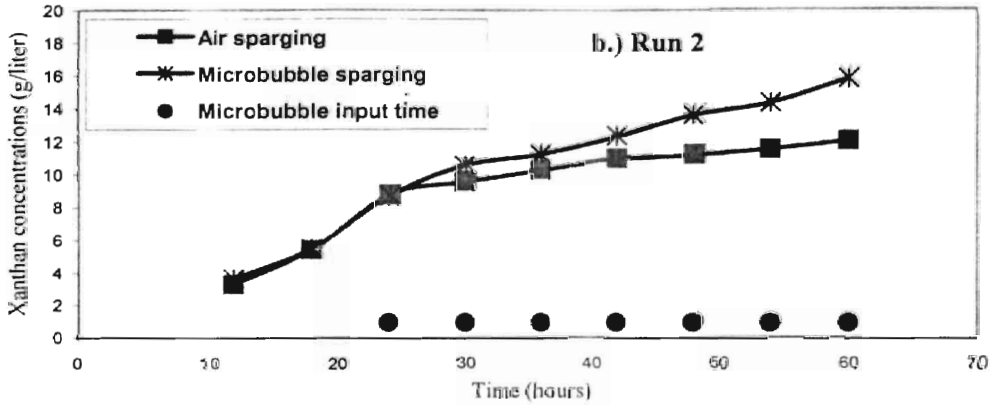

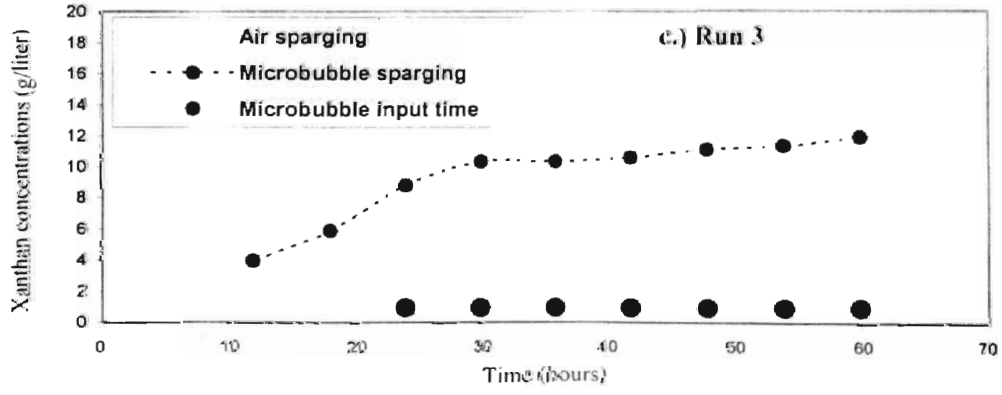

Figure 22. Xanthan yields with time for air and partially substituted microbubble sparging fermentation experiments (6L) for a.) Run 1, b.) Run 2, and c.) Run 3

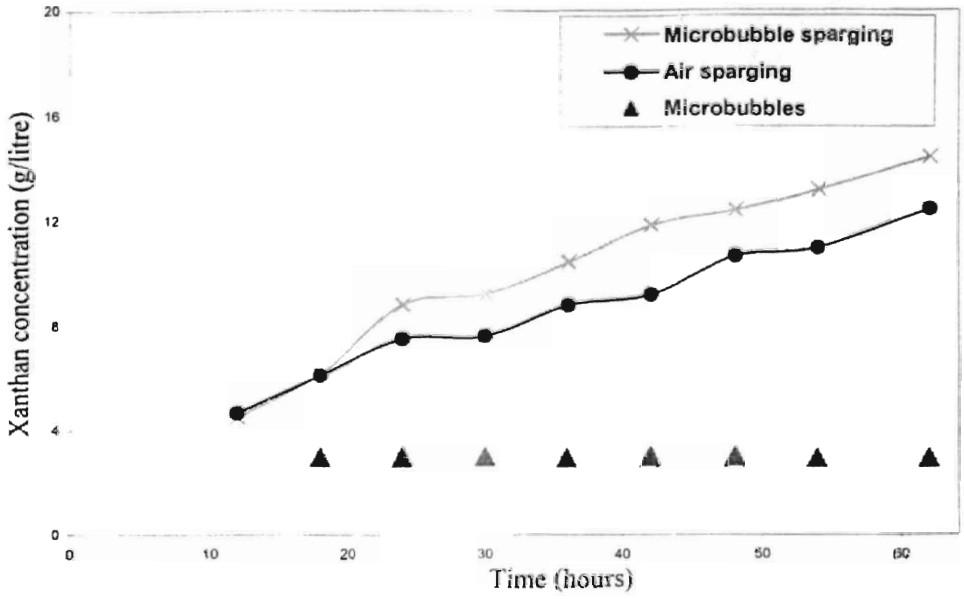

Figure 23. Xanthan trends with time for air and partially substituted microbubble sparging fed batch experiments

Effect of Microbubbles on OUR, SPOUR and K_La values

Figure 24 shows the oxygen uptake rate (OUR) profiles for fermentation runs utilizing air and microbubble sparging approaches obtained by the dynamic method. A comparison of OUR values for both approaches shows that microbubble substitution increased the OUR in cells. OUR values ranged from as high as 5, 7 and 9 mol O_2 / m^3-h (in the peak exponential phase) to 2.5, 2.25 and 2.5 mol O_2 / m^3-h (at the end of run) for the microbubble approach in comparison to 3.5, 6 and 5.9 mol O_2 / m^3-h (in the peak phase) to 1.35, 1 and 0.8 mol O_2 / m^3-h (at the end) for air sparging. The significant difference in OUR between the two approaches can be clearly seen in Figure 24. Similar results involving increased OUR were observed in fed-batch experiments, and are shown in Figure 25.

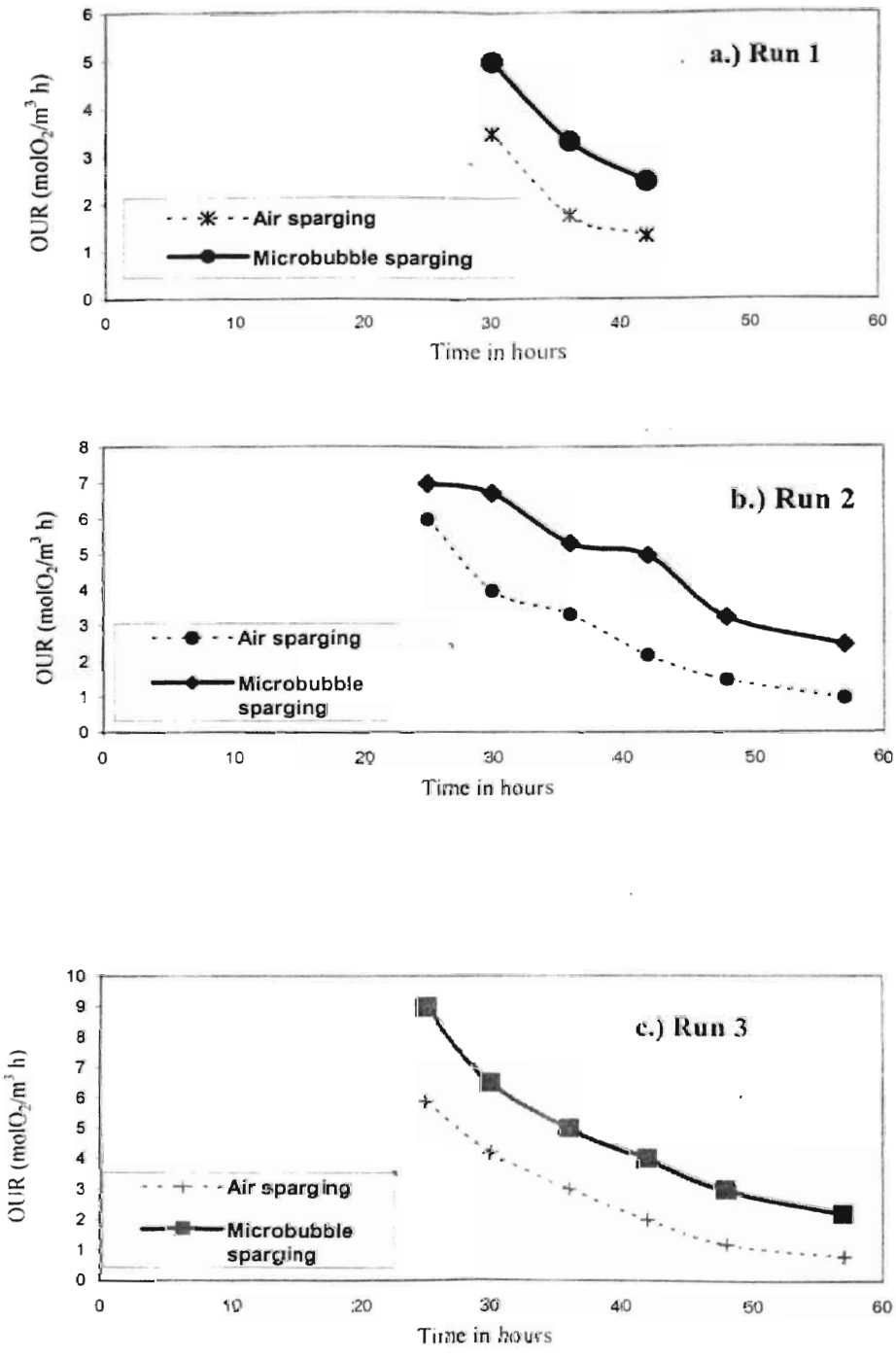

Figure 24. Oxygen uptake rate (OUR) comparisons with time for air and partially substituted microbubble sparging fermentation experiments for a.) Run 1, b.) Run 2, and c.) Run 3

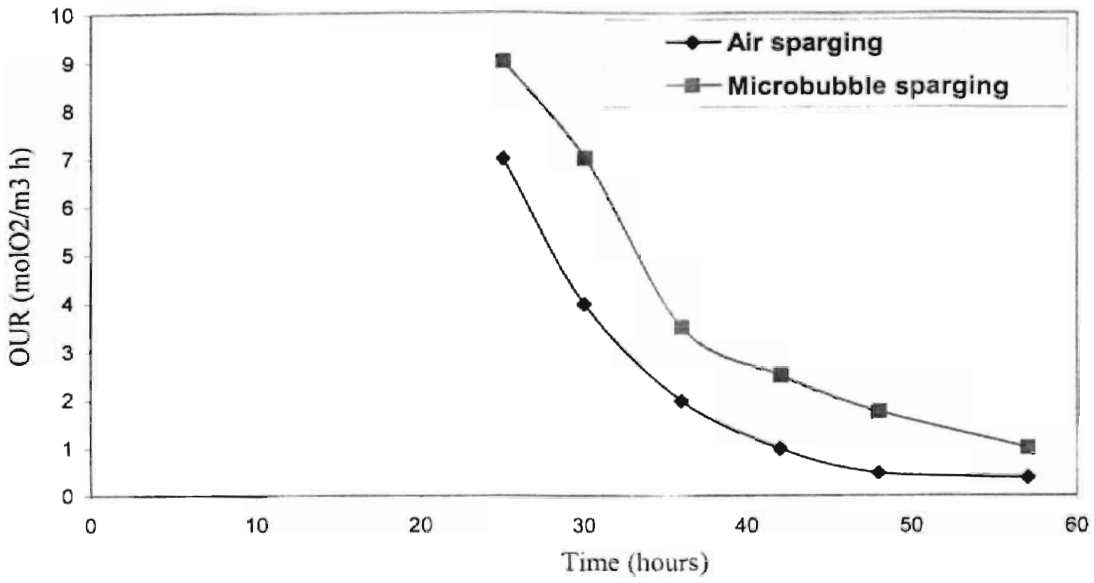

Figure 25. Oxygen uptake rate comparisons with time for air and partially substituted microbubble sparging fed-batch fermentation experiments

Fermentation runs involving microbubbles had OUR values ranging from 9 mol O_2 / m^3-h (in the peak exponential phase) to 1 mol O_2 / m^3-h (at the end of run) in comparison to air sparing fermentations with values ranging from 7 mol O_2 / m^3-h to 0.4 mol O_2 / m^3-h.

The increase in OUR with microbubbles can be attributed to the smaller size of the bubbles, enabling larger interfacial areas and better oxygen transfer resulting in increased OUR by microorganisms. Pramuk (2000) also observed similar effects of microbubbles in yeast fermentations, reporting OUR values (by the yield coefficient method) of 127 m mol O_2 / m^3-h and 137 m mol O_2 / m^3-h for microbubble sparging in comparison to 64 m mol O_2/ m^3-h and 76 m mol O_2 / m^3-h for air sparging in 1-L and 50-L working volume fermentation experiments. Our

trends involving oxygen uptake rate for microbubble sparging are very similar to the earlier results of Pramuk.

Specific oxygen uptake rate (SPOUR), which is OUR divided by biomass concentration, was calculated and profiles plotted to compare the trends for air and microbubble sparging experiments. Figure 26 shows the SPOUR profile comparisons for air and partially substituted microbubble-sparging fermentations. SPOUR values for microbubble sparging experiments ranged as high as 3.11, 4.24 and 3.45 mol O_2 / gram of biomass-h (in the peak exponential phase) to 1.33, 1.1 and 0.87mol O_2 / gram of biomass-h (at the end of run) in comparison to air sparing fermentations with values ranging from 2.18, 3.75 and 2.62 mol O_2 / gram of biomass-h to 0.77, 0.48 and 0.25 mol O_2 / gram of biomass-h. The higher SPOUR trends in the microbubble sparging experiments confirm the effect of microbubbles in enhancing OUR, causing both an increase in biomass concentration and an increase in OUR. Similar results of higher SPOUR were observed in fed batch experiments, as shown in Figure 27. Values ranged from 6.48 to 0.5 mol O_2 / gram of biomass-h for microbubble sparging experiments in comparison to 4.95 mol O_2 / gram of biomass-h (in the peak exponential phase) to 0.24 mol O_2 / gram of biomass-h (at the end of run).

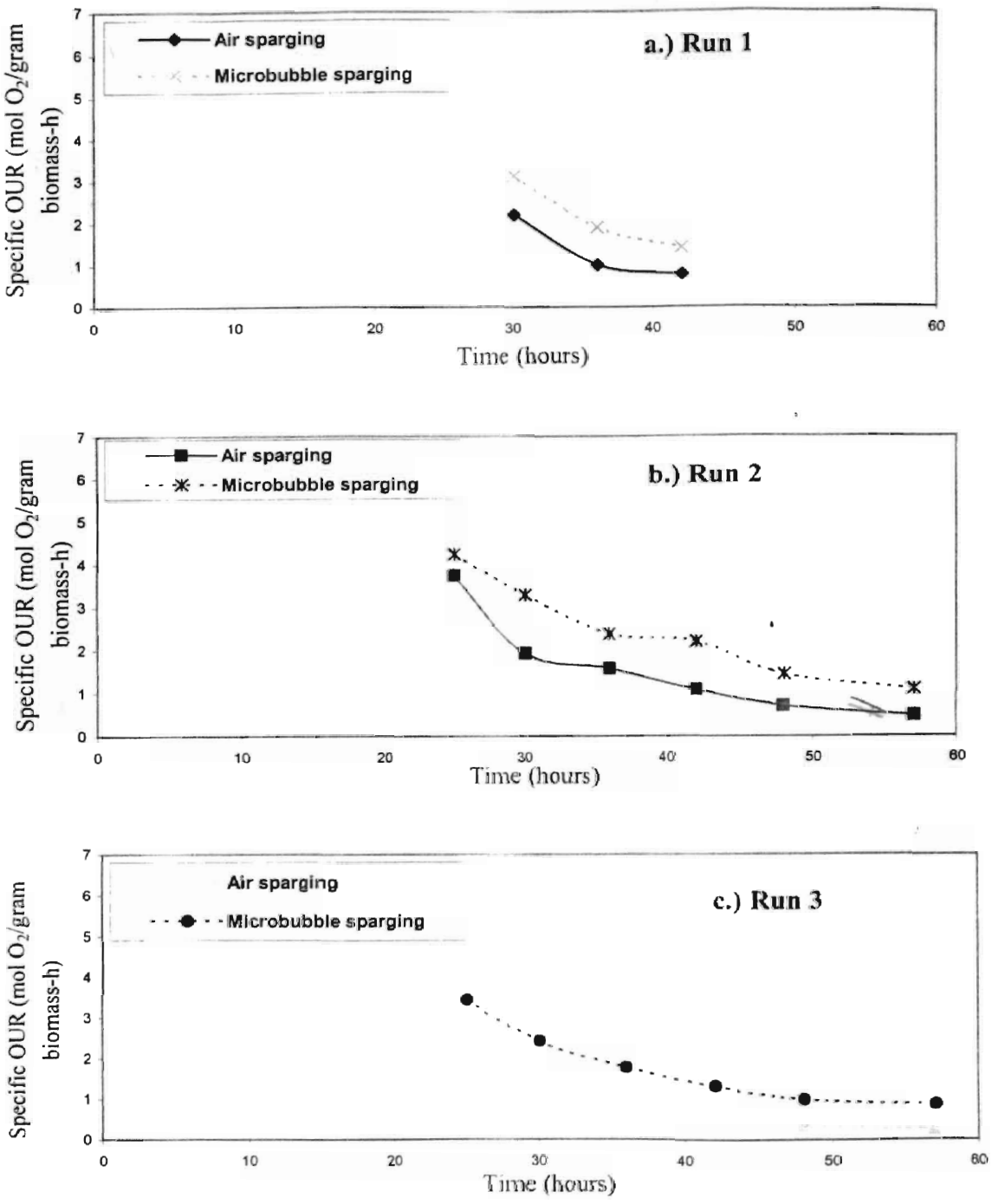

Figure 26. Specific oxygen uptake rate trends with time for air and partially substituted microbubble sparging fermentations for a.) Run 1, b.) Run 2, and c.) Run 3

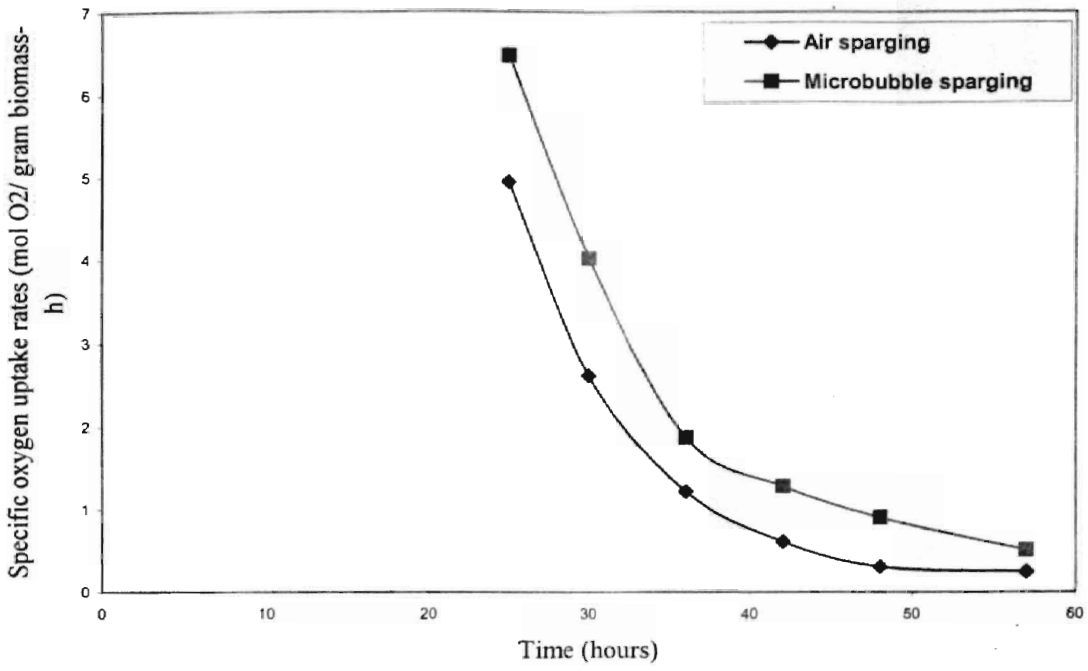

Figure 27. Specific oxygen uptake rate trends with time for air and partially substituted microbubble sparging fed batch fermentation experiments

Oxygen transfer rate is generally expressed as volumetric mass transfer coefficient in fermentation mass transfer studies. It is calculated by dynamic method by monitoring the rate of increase in dissolved oxygen concentration with time and fitting the values in the integral form of mass balance equation for batch fermentation derived as in Garcia et al, 2000. Figure 28 presents the profile of volumetric mass transfer coefficient (K_La) with time for air and microbubble sparging experiments. It can be seen from these profiles that volumetric mass transfer coefficient values ranged from 0.0024, 0.0011 and 0.0021 1/s (in the peak exponential phase) to 0.002, 0.0009 and 0.0018 1/s (at the end of run) for

microbubble sparging in comparison to 0.000947, 0.0011 and 0.0010 1/s (in the peak exponential phase) to 0.0009, 0.00033 to 0.00034 1/s for air sparging. Similarly, from the results of fed batch experiments presented in Figure 29, it was noticed that volumetric mass transfer coefficient values ranged as high as 0.00096 1/s (in the peak exponential phase) to 0.0012 1/s (at the end of run) for microbubble sparging in comparison to 0.00068 1/s and 0.00027 1/s for air sparging experiments.

The higher K_La values can be attributed to the smaller size of microbubbles in the fermenter, resulting in larger interfacial areas (~15-30 times larger in comparison to air sparging). Microbubbles thereby facilitate higher K_La values in comparison to air sparging, resulting in a higher degree of oxygen transfer in the fermenter. Kaster, 1990 reported a four-fold increase in K_La values with the use of microbubble sparging in comparison to air sparging in yeast fermentation experiments. Bredwell and Worden, 1998 also reported a 6-fold increase in K_La values with the use of microbubble sparging at half the flow rates in comparison to air sparging in synthesis gas fermentations, explaining the potential of microbubbles in enhancing oxygen transfer in fermentations. Recently, Pramuk (2000) also reported that microbubble sparging in yeast fermentations at agitation speeds of 150 rpm resulted in a two-fold increase in K_La in comparison to air sparging K_La values in both 1-L and 50-L fermentation experiments. The increased oxygen transfer rates experienced with the introduction of microbubbles enables effective oxygen utilization, increasing OUR & SPOUR values, thus resulting in higher biomass and xanthan yields.

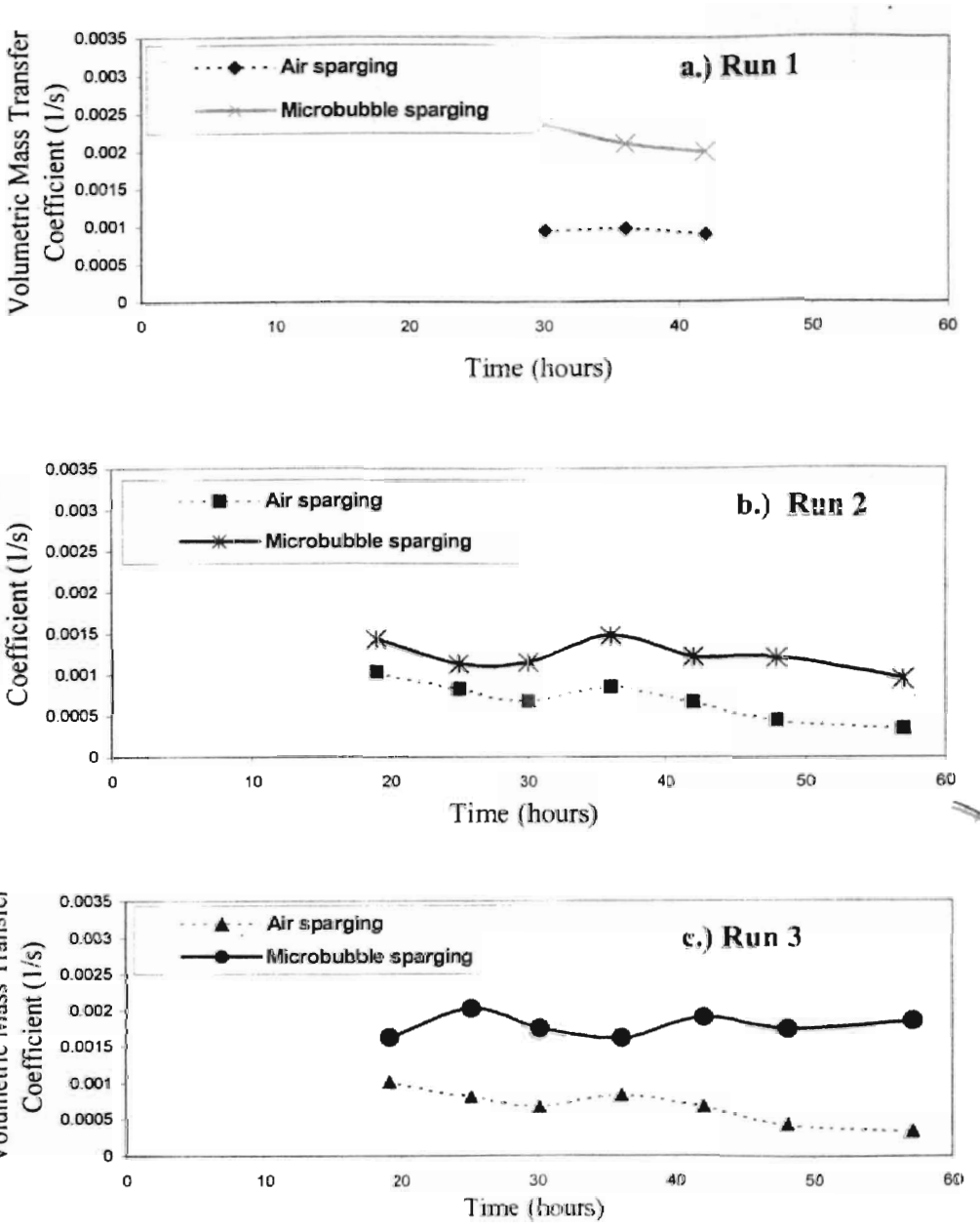

Figure 28. Volumetric mass transfer coefficient with time for air and partially substituted microbubble sparging experiments for a.) Run 1, b.) Run 2, and c.) Run 3

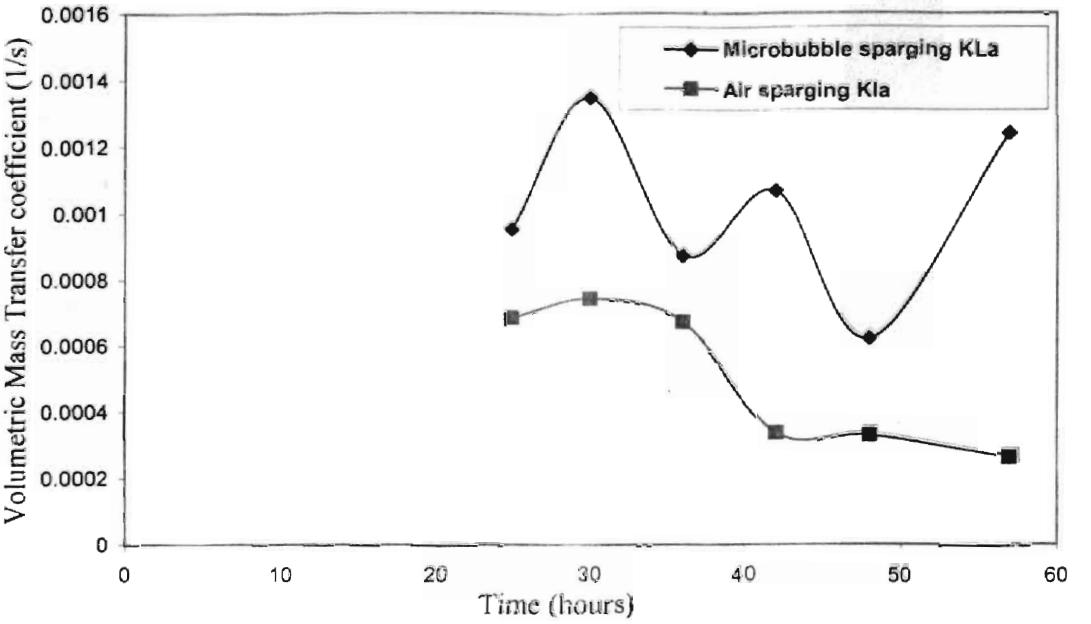

Figure 29. Volumetric mass transfer coefficient with time for air and partially substituted microbubble sparging fed batch experiments

Effect of Air and Microbubble Sparging Runs on Xanthan Quality

In order to verify whether shear force in the microbubble generator had any effect on final xanthan quality, HPLC studies involving molecular weight distribution comparisons between air and microbubble derived final xanthan samples were conducted. Results from HPLC tests are shown in Appendices A.9 & A.10. From that data, it can be seen that the shear had no effect on molecular weight of xanthan, as both peaks have identical retention times of 19.968 minutes. Further, the values of the HPLC indices for control and microbubble derived xanthan samples were; base line start: 19.050 vs. 19.117 minutes, base line end: 20.9 vs. 20.783 minutes; height being 88913 vs. 89035; width being 111

vs. 100 seconds; and area of peaks being 2374212 vs. 2373184 units. A comparison of these chromatograms based on HPLC indices indicates that shear in the microbubble generator had no significant effect on the final xanthan quality.

Similarly xanthan samples derived from fed-batch fermentation experiments were analyzed on the HPLC and comparisons were made between air and microbubble derived final xanthan samples. Again shear force seemed to have little effect on the molecular weight of xanthan, as all HPLC indices were very similar. All of these results support hypothesis that the xanthan molecule is resistant to the shearing conditions within the microbubble generator.

Microbubble Properties during Fermentation Experiments

During both 6-L and 4+2L fed-batch fermentation runs, gas-hold-up values during microbubble sparging experiments were obtained to know the degree of air content achieved in the microbubble generator and to compare the actual values with the values derived from preliminary experiments with model solutions. The trends in both types of fermentation runs are very similar to the model solutions, as seen in Figure 30. The gas-hold-up values ranged from 65% at 24 hours to 52% at 54 hours. The decrease in air content with time can be attributed to the increasing viscosity of broth with time, due to production of xanthan by the microorganisms.

It is hypothesized that the gas-hold-up could be increased with the use of multiple spinning discs in the microbubble generator. The current microbubble

generator design contains only one. This could further improve the oxygen transfer properties in fermenter.

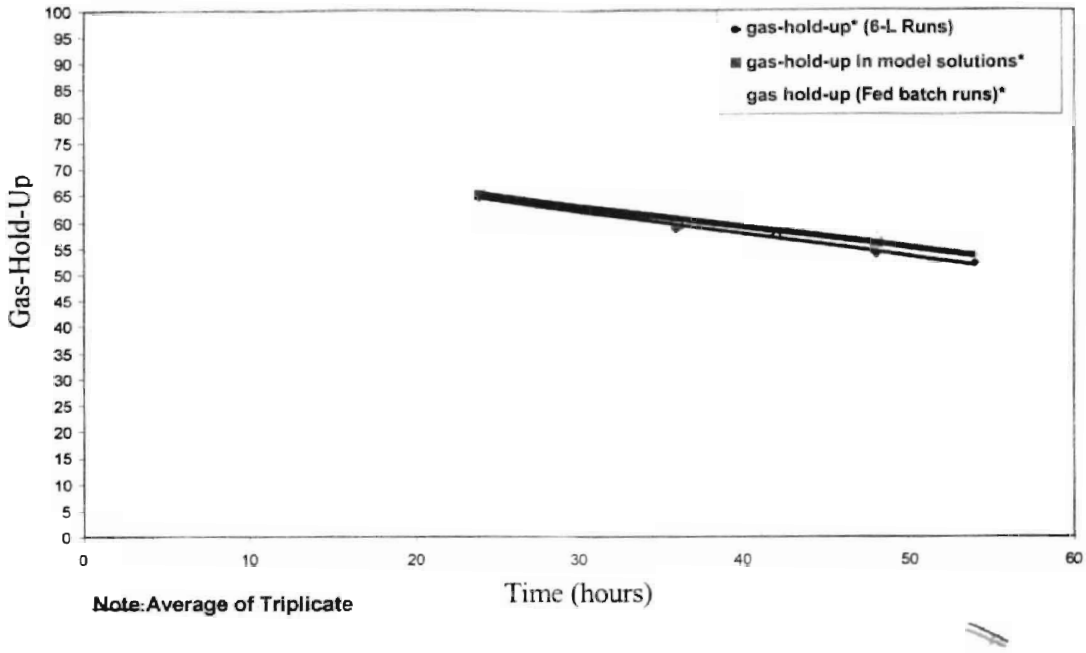

Figure 30. Gas-hold-up comparisons for microbubble runs and model solutions

Energy Consumption

Energy consumption comparisons were made for fermentation runs utilizing air and microbubble sparging. Figure 31 shows energy consumption along with xanthan yield for each comparative run. The net energy consumption values include all energy required except that of the air compressor for both the approaches. So values shown for air sparging refer to the energy required by the fermenter, while for microbubble sparging it included energy required by the fermenter, microbubble generator and the two circulating pumps. From Figure 31

it can be seen that net energy consumption for air sparging runs were 26.723, 33.125 and 31.525 kWh, corresponding to a final xanthan yields of 11.85, 12.14 and 9.52 g/l respectively. In comparison, microbubble-sparging runs had net energy consumption values of 27.5, 39.723 and 35.148 kWh corresponding to final xanthan yields of 13.24, 15.92 and 12 g/l. The energy requirements for microbubble sparging experiments included approximately 1.2 kWh of energy consumption for the microbubble generator & circulating positive displacement pumps for the entire 60-hour run, which represents a relatively small amount of energy.

Although the energy consumption for microbubble sparging experiments was higher than air sparging experiments, the energy consumed per gram of xanthan yield with the microbubble approach was less than that for air sparging experiments. The energy consumption per gram of xanthan produced for microbubble substituted experiments were 2.08, 2.49 and 2.63 kWh/g xanthan

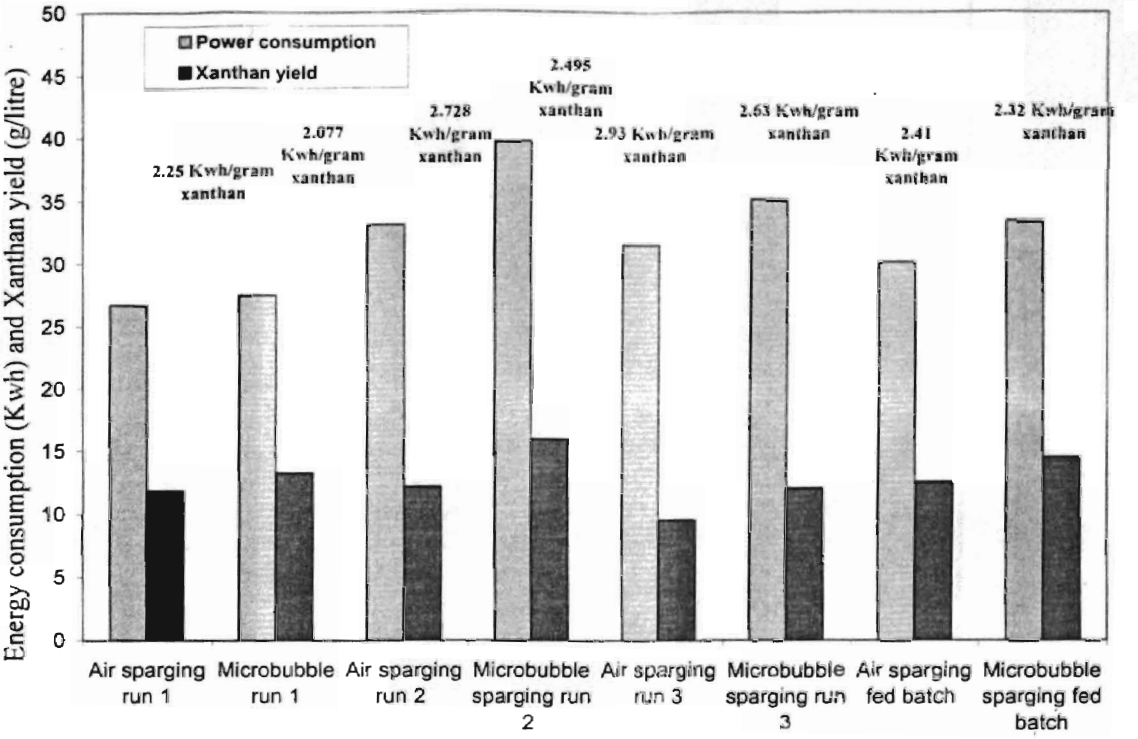

Figure 31. Power consumption and Xanthan yield comparisons for Air and partially substituted Microbubble sparging fermentation experiments

compared to air sparging experiment values of 2.25, 2.73 and 2.93 kWh/g xanthan. This amounts to an average savings of 0.236 kWh/g of xanthan with the use of microbubbles in 6-L xanthan fermentations. This savings in energy per unit weight of xanthan demonstrates the advantages microbubbles offer in reducing the energy requirements for existing air sparging fermentation systems.

Earlier researchers also reported similar results of savings in energy consumption due to enhanced mass transfer with the use of microbubble sparging in fermentation studies. Pramuk (2000) reported a 3-fold reduction in energy consumption in 50-L yeast fermentations operated at 150 rpm to achieve similar final biomass yields as achieved with air sparging fermentations.

Hensirisak (1997) reported that with the use of microbubble sparging in yeast fermentations, energy savings of 68% and 55% for 50-L and 20-L fermentations at 150 rpm were achieved. Although our savings were less than the reported values for yeast fermentations because of small working volumes for our experiments in comparison to literature, it can be hypothesized that with scale-up, similar substantial savings in energy consumption requirements for xanthan gum fermentations could be realized.

CHAPTER V

CONCLUSIONS

The results of this study suggest that microbubble substitution in xanthan fermentation can be used to achieve increased oxygen mass transfer and hence increased biomass and xanthan yields and energy consumption savings in xanthan fermentations. The following specific conclusions were drawn from this study:

1. *X.Campestris* is biocompatible with Tween-20 surfactant at surfactant levels of 0-500 ppm.
2. Gas hold-up and foam stability of microbubbles ranged from 20% to >78.6 % and 0.3 to >5 minutes, respectively, for the following range of operating conditions within the microbubble generator: agitation speed 5,000-8,000 rpm, surfactant levels 120, 300, & 500 ppm, and process time 2-5 minutes.
3. *X.Campestris* organisms were found to be resistant to shear in the microbubble generator at an agitation speed of 8,000 rpm, a surfactant level of 300 ppm, and a process time of 2 minutes.
4. Xanthan gum quality was not affected by the shear force encountered in the microbubble generator at the conditions tested.
5. Microbubble size distributions ranged from 120 to 400 μ during microbubble substitution into the fermenter. The increase in size is attributed to increasing viscosity of the media due to xanthan production.

6. Experiments involving microbubble substitution for ½ hour intermittently at 6-hour intervals had a higher oxygen uptake rate, specific oxygen uptake rate, and volumetric mass transfer coefficient values in comparison with air sparging runs.
7. Microbubble substitution increased biomass and xanthan levels up to ~20% and ~30%, respectively, in 6-L fermentation runs.
8. Increased mass transfer and hence final xanthan yield with microbubble sparging enabled more energy efficient xanthan production (2.4 kWh/g against 2.64 kWh/g of xanthan) for microbubble sparging experiments in comparison to air sparging experiments.

CHAPTER VI

RECOMMENDATIONS FOR FUTURE WORK

This study focused on determining whether the microbubbles are effective in improving oxygen mass transfer during viscous fermentations for a particular set of fermenter and microbubble generator operating conditions. However, further studies are necessary to evaluate the potential microbubbles offer for a wide range of fermenter and microbubble generator operating conditions and to explore the extent of improvements in mass transfer and yield that could be achieved. In particular, the extent and frequency of substitution of microbubbles into the fermenter could be further optimized.

The microbubble generator used in this study was a single spinning disc generator. This resulted in a drop in gas-hold-up and an increase in microbubble size due to increased viscosity with time of fermentation. A potential solution is to add multiple discs in the generator and to see if the properties can be consistently delivered throughout the microbubble solution.

These studies were conducted in a 14-L fermenter with a 6-L working volume and there is a need for scale-up studies to see the extent of improvement in mass transfer, yield and energy consumption savings that could be achieved with the use of microbubbles at larger volumes.

One additional potential area of further research is to explore incorporation of the microbubble generator within the fermenter and determine whether similar

benefits could be realized without the need for pumping the broth from outside the fermenter.

REFERENCES

Albrecht, W.J., V.E. Sohns, and S.P. Rogovin.1963. Biotechnology and Bioengineering. 5: 91.

Amanullah, A., L. Serrano-Carren, B. Castro, E. Galindo, and A.W.Nienow, 1998. The influence of impeller type in pilot scale xanthan fermentations. Biotechnology and Bioengineering. 57(1): 95-108.

Atkinson, B. and F. Mavituna.1991. Biochemical Engineering and Biotechnology Handbook, 2nd edition. Stockton press, New York.

Bailey, J.E., and D.F. Ollis. 1986. Biochemical Engineering Fundamentals. 2nd edition. McGraw-Hill Book Company, New York.

Bredwell, M.D., M.D. Telgenhoff, and R.M. Worden. 1995. Formation and coalescence properties of microbubbles. Applied Biochemistry and Biotechnology. 52: 501-509.

Bredwell, M.D., M.D. Telgenhoff, S. Barnard and R.M. Worden. 1997. Effect of surfactants on carbon monoxide fermentations by butyribacterium methylotrophicum. Applied Biochemistry and Biotechnology. 63-65: 637-647.

Bredwell, M.D., and R. M. Worden. 1998. Mass Transfer Properties of Microbubbles. 1. Experimental Studies. Biotechnological Progress. 14: 31-38.

Chapalkar, P.G., K.T. Valsaraj, and D. Roy. 1993. Separation Science Technology. 28: 1287-1302.

Cooper, C.M., G.A. Fernstorm, and S.A. Miller. 1944. Performance of agitated gas-liquid contractors. Industrial Engineering Chemical. 36(6): 504-509.

Cottrell, W.I and S.K. Kang. 1978. Xanthan gum. A unique bacterial polysaccharide for food applications. Developments in Industrial Microbiology. 19:177.

De Vries, A.J. 1972. In Adsorptive Bubble Separation Techniques (Lemlich, R., edition), pp. 7-31, Academic press.

De Vuyst, L., J.VanLoo, and E.J., Vandarme. 1987. Two step fermentation process for improved xanthan production by X. Campestris NRRL B1459. Journal of Chemical Technology and Biotechnology. 39: 263-273.

Doran, P.M. 1995. Bioprocess Engineering principles. Academic Press, San Diego.

Dussap, C.G., J. Decorps, and J.B. Gros. 1985. Transfert d' oxygene en presence de polysaccharide exocellulaires dans un fermenteur agite aere et dans un fermenter de type gazosiphon. Entropie. 123: 11-20.

Fletcher, S.I. 1994. A study of the mixing, oxygen mass transfer and power consumption in and rheology of non-newtonian fermentations. PhD Thesis, University of Birmingham, UK.

Funahashi, H., K.I. Hirai, T.Yoshida, and H.Taguchi. 1988a. Mixing state of xanthan gum solution in aereated and agitated fermenter-effects of impeller size on volumes of mixed regions and circulation time distribution. Journal of Fermentation Technology. 66: 103-109.

Funahashi, H., K.I Hirai, T.Yoshida, and H.Taguchi. 1988b. Mechanistic analysis of xanthan gum production in a stirred tank. Journal of Fermentation Technology. 3: 335-364.

Funahashi, H., M.Machara, H.Taguchi, and T. Yoshida.1987b. Effects of agitation by flat bladed turbine impeller on microbial production of xanthan gum. Journal of Chemical Engineering (Japan). 20:16-22.

Funahashi, H., T.Yoshida, and H.Taguchi. 1987a. Effect of glucose concentration on xanthan gum production by Xanthomonas Campestris. Journal of Fermentation Technology. 65: 603-606.

Funahashi, H., K.I. Hirai, T.Yoshida, and H.Taguchi.1988. Mechanistic analysis of xanthan gum production in a stirred tank. Journal of Fermentation Technology. 66: 355-364.

Galindo, E. 1994. Aspects of the process of xanthan production. Transactions of IChemE. 72: Part C, 227-237.

Galindo, E. 1985. Polisacaridos Microbianos. In Perspectives de la Biotechnologia en Mexico, ed. R. Quintero. CONACYT-FJBS, A.C., Mexico.D.F. pp. 65-92.

Garcia-Ochoa, F., E. Gomez Castro, and V.E. Santos. 2000. Oxygen transfer and uptake rates during xanthan production. Enzyme and Microbial Technology. 27: 680-690.

Garcia-Ochoa, F., and E.Gomez. 1998. Mass transfer coefficient in stirred tank reactors for xanthan solutions. Biochemical Engineering Journal. 1: 1-10.

Hensirisak, P. 1997. Scale-up the use of a microbubble dispersion to increase oxygen transfer in aerobic fermentation of baker's yeast. MS Thesis, Virginia Polytechnic Institute and State University. Blacksburg, Virginia.

Jauregi P, and Varley, J. 1999. Colloidal gas aphrons: potential applications in biotechnology. In: Trends in Biotechnology, Jaargang. 17: 389-395.

Jauregi, P., S. Gilmour, and J. Varley. 1997. Characterization of colloidal gas aphrons for subsequent use for protein recovery. Chemical Engineering Journal. 65:1-11.

Kaster, J.A., D.L. Michelson, and W.H. Velander.1990. Increased oxygen transfer in yeast fermentation using a microbubble dispersion. MS Thesis, Virginia Polytechnic Institute and State University. Blacksburg, Virginia.

Kennedy, J.F. and I.J.Bradshaw. 1984. Production, properties and application of xanthan. Progress Industrial Microbiology. 19: 319-371.

Kommalapati, R.R., D. Roy, K.T. Valsraj, and W.D.Constant. 1996. Separation Science Technology. 31: 2317-2333.

Liakopoulov-kyriakides, M., E.S. Tzanakakis, C. Kiparissidis, L.V. Ekaterianiadou and D.A. Kyriakidis.1997. Kinetics of xanthan gum production from whey by constructed strains of X. Campestris in batch fermentations. Chemical Engineering Technology. 20: 354-60.

Linek, V. and V. Vacek. 1988. Volumetric mass transfer coefficient in stirred reactors. Chemical Engineering Technology. 11: 249-51.

Margaritis, A and G.W. Pace. 1985. In: Moo-Young, M, editor. Comprehensive Biotechnology. Vol. 3. Toranto: Pergamon. 1005-1043.

Marquet, M., M. Mikolajczak, L. Thorne, and T.J. Pollock. 1989. Improved strains for the production of xanthan by fermentation of Xanthomonas Campestris. Journal of Industrial Microbiology. 4: 55-64.

Matsushita, K., A.H. Mollah, D.C. Stuckey, C. Del Cerro, and A.I. Bailey.1992. Colloidal Surface. 69: 65-72.

Moraine, R.A. and P.Rogovin. 1971. Xanthan biopolymer production and increased concentration by pH control. Biotechnology and Bioengineering.13: 381-391.

Moraine, R.A. and P. Rogovin. 1973. Biotechnology and Bioengineering. 15: 225.

Moser, A. 1966. Oxygen transfer and microbial growth. In Computer and Information Science Application in Bioprocess Engineering, ed. A.R. Moreira and K.K. Wallace, 377-394. Kluwer Academic Publishers, Dordrecht.

Motarjemi, M. and G.J. Jameson. 1978. Mass transfer from very small bubbles - the optimum bubble size for aereation. Chemical Engineering Science. 33(11): 1415-1423.

Nienow, A.W.1984. Mixing studies on high viscosity fermentation process-xanthan gums. World Biotech Report 1: 293-304. (Europe online publications, UK).

Nishikawa, M., M. Nakumara, and K. Hashimoto. 1981. Gas absorption in aereated mixing vessels with non-Newtonian liquid. Journal of Chemical Engineering (Japan). 14(3): 227-32.

Nokajim, S., H.Funahashi, and T.Yoshida. 1990. Xanthan gum production in a fermenter with twin impellers. Journal of Fermentation and Bioengineering. 70: 392-397.

Pace, G.W., R.C.Righelato. 1980. Production of extracellular microbial polysaccharide. Advances in Biochemical Engineering. 15:1-70.

Pace, G.W. 1987. In: Kristiansen, B, Bu'lock, J, editors. Basic Biotechnology. London: Academic Press. 449-62.

Peters, H.U., Suh, I.S., Schumpe, A., and W.D. Deckwer. 1992. Modeling of batchwise xanthan production. Canadian Journal of Chemical Engineering. 70: 742-750.

Peters, H.V., H. Herbst, P.G.M. Heselink, H. Lunsdorf, A. Schumpe, and W.D.Deckwer. 1989. The influence of agitation rate on xanthan production by X. Campestris. Biotechnology and Bioengineering. 34: 1393-1397.

Pramuk, P. 2000. Utilization of microbubble to increase oxygen transfer in pilot scale bakers yeast fermentation unit. MS Thesis, Virginia Polytechnic Institute and State University. Blacksburg, Virginia.

Richard, J.W. 1961. Studies in aereation and agitation. Progress in Industrial Microbiology. 3:143-172.

Rogovin, S.P., R.F. Anderson, and M.C Cadmus. 1961. Production of polysaccharides with Xanthomonas Campestris. Journal of Biochemistry and Microbiological Technology Progress. 4: 231-241.

Roy, D., K.T. Valsaraj, and S.A.Kottai. 1992. Separation Science Technology. 25: 573-588.

Save, S.V. and V.G. Pangarkar. 1994. Chemical Engineering Communication. 127: 35-53.

Sebba, F. 1971. Microfoams - an unexploited colloid system. Journal of Colloid Interface Science. 35(4): 643-646.

Sebba, F.1985. An improved generator for micron-size bubbles. Chemical Industry (London). 4: 91-92.

Sebba, F. 1987. Foams and Biliquid Foams-Aphrons, John Wiley and Sons, New York.

Shaw, D.J. 1992. Introduction to Colloid and surface Chemistry (4th edition), Buttersworth-Heinemann.

Shu, C.H. and S.T.Yang. 1990. Effects of temperature on cell growth and xanthan production in batch culture of Xanthomonas Campestris. Biotechnology and Bioengineering. 13: 454-468.

Soloman, J., T.P. Elson, A.W.Nienow, and G.W Pace. 1981a. Cavern sizes in agitated fluids with a yield stress. Chemical Engineering Communication. 11: 143-164.

Souw, P. and A.L. Demain. 1979. Nutritional studies on xanthan production by Xanthomonas Campestris NRRL B1459. Applied Environmental Microbiology. 37, 1186-1192.

Stanbury, P.F., A. Whitaker, and S.J. Hall. 1995. Principles of Fermentation technology, 2nd edition. New York: Elsevier Science Ltd.

Suh, I.S., J. Herbst, A.Schumpe, and W. D. Deckwer. 1990. The molecular weight of xanthan polysaccharide produced under oxygen limitation. Biotechnology Letters. 12: 201-206.

Taguchi, H. and A.E. Humphrey. 1966. Dynamic measurement of volumetric oxygen transfer coefficient in fermentation system. Journal of Fermentation Technology in Japan. 44: 881-889.

Tecante, A, and L.Choplin. 1993. Gas-liquid mass transfer in Non-Newtonian fluids in a tank stirred with a helical ribbon screw impeller. Canadian Journal of Chemical Engineering. 71: 859-65.

Wallis, D.A., S.R.Lavinder, D.L.Michelsen, and F.Sebba.1986. A novel bioprocess for high oxygen transfer in tower bioreactors. Paper presented at the 1986 Summer National Meeting of the American Institute of Chemical Engineers, Boston MA.

Wang, D.I.C., C.I. Cooney, A.L. Demain, P. Dunnill, A.E. Humphrey, and M.D. Lilly. 1971. Fermentation and Enzyme Technology. New York: John Wiley & Sons.

Worden, R.M., and M.D. Bredwell. 1998. Mass-Transfer properties of Microbubbles. 2. Analysis using a dynamic model. Biotechnological Progress. 14: 39-46.

Yagi, H, and F. Yoshida. 1975. Gas absorption by newtonian and non-newtonian fluids in sparged agitated vessels. Industrial Engineering Chemical Process Design and Development. 14: 488-493.

APPENDIX

Sample Report

Reported by User: System

Project Name: XanthanJan92003

SAMPLE INFORMATION

Sample Name:	C05S0	Acquired By:	System
Sample Type:	Unknown	Date Acquired:	2/5/2003 6:24:43 PM
Vial:	86	Acq. Method Set:	Xanthan New
Injection #:	1	Date Processed:	2/7/2003 3:53:28 PM
Injection Volume:	100.00 ul	Processing Method:	Xanthan Calibration Final
Run Time:	25.0 Minutes	Channel Name:	410
Sample Set Name:	XanFeb03	Proc. Chnl. Descr.:	

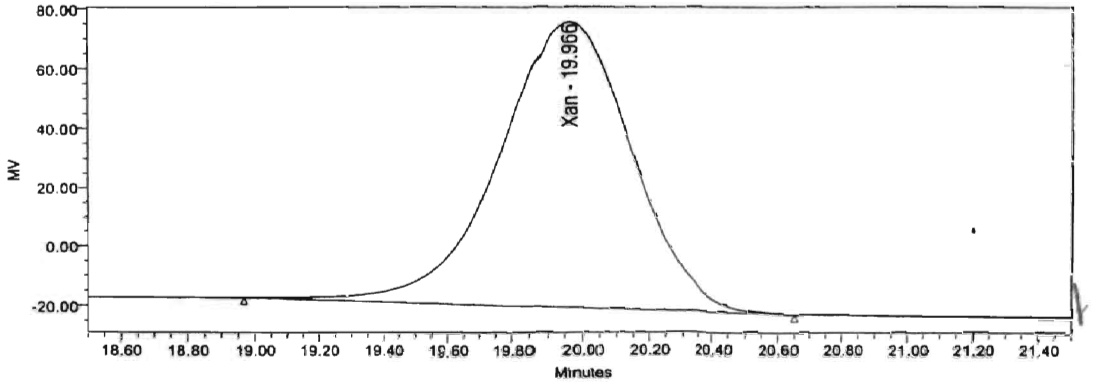

	RT	% Area	Area	Width (sec)	Height	Units	Baseline Start (min)
1	19.966	100.00	2633788	101.000	96305	micro gm	18.967

	Baseline End (min)	Offset (µV)	Slope (µV/sec)
1	20.650	4.679479e+001	-3.381338e+000

Sample Report

Reported by User: System

Project Name: XanthanJan92003

SAMPLE INFORMATION

Sample Name:	C05S5	Acquired By:	System
Sample Type:	Unknown	Date Acquired:	2/5/2003 6:51:08 PM
Vial:	87	Acq. Method Set:	Xanthan New
Injection #:	1	Date Processed:	2/7/2003 3:53:28 PM
Injection Volume:	100.00 ul	Processing Method:	Xanthan Calibration Final
Run Time:	25.0 Minutes	Channel Name:	410
Sample Set Name:	XanFeb03	Proc. Chnl. Descr.:	

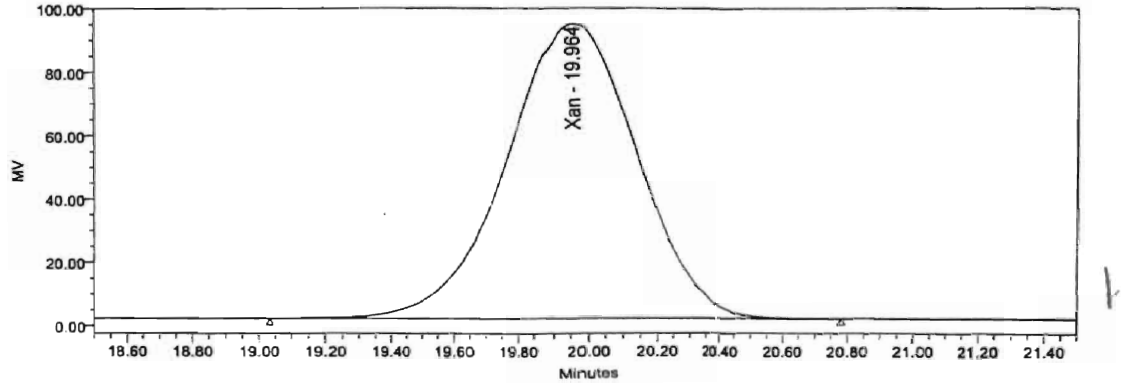

	RT	% Area	Area	Width (sec)	Height	Units	Baseline Start (min)
1	19.964	100.00	2476671	105.000	93155	micro gm	19.033

	Baseline End (min)	Offset (µV)	Slope (µV/sec)
1	20.783	2.316442e+000	-2.674772e-003

Sample Report

Reported by User: System

Project Name: XanthanJan92003

SAMPLE INFORMATION

Sample Name:	C05S10	Acquired By:	System
Sample Type:	Unknown	Date Acquired:	2/5/2003 7:17:34 PM
Vial:	88	Acq. Method Set:	Xanthan New
Injection #:	1	Date Processed:	2/7/2003 3:53:28 PM
Injection Volume:	100.00 ul	Processing Method:	Xanthan Calibration Final
Run Time:	25.0 Minutes	Channel Name:	410
Sample Set Name:	XanFeb03	Proc. Chnl. Descr.:	

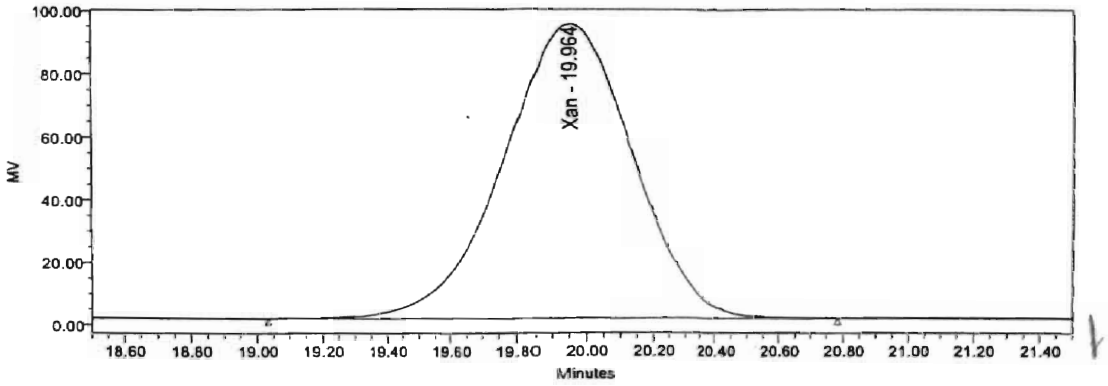

	RT	% Area	Area	Width (sec)	Height	Units	Baseline Start (min)
1	19.964	100.00	2486360	105.000	93554	micro gm	19.033

	Baseline End (min)	Offset (µV)	Slope (µV/sec)
1	20.783	2.750067e+000	-3.209726e-002

Sample Report

Reported by User: System

Project Name: XanthanJan92003

SAMPLE INFORMATION

Sample Name:	C05S15	Acquired By:	System
Sample Type:	Unknown	Date Acquired:	2/5/2003 7:43:59 PM
Vial:	89	Acq. Method Set:	Xanthan New
Injection #:	1	Date Processed:	2/7/2003 3:53:27 PM
Injection Volume:	100.00 ul	Processing Method:	Xanthan Calibration Final
Run Time:	25.0 Minutes	Channel Name:	410
Sample Set Name:	XanFeb03	Proc. Chnl. Descr.:	

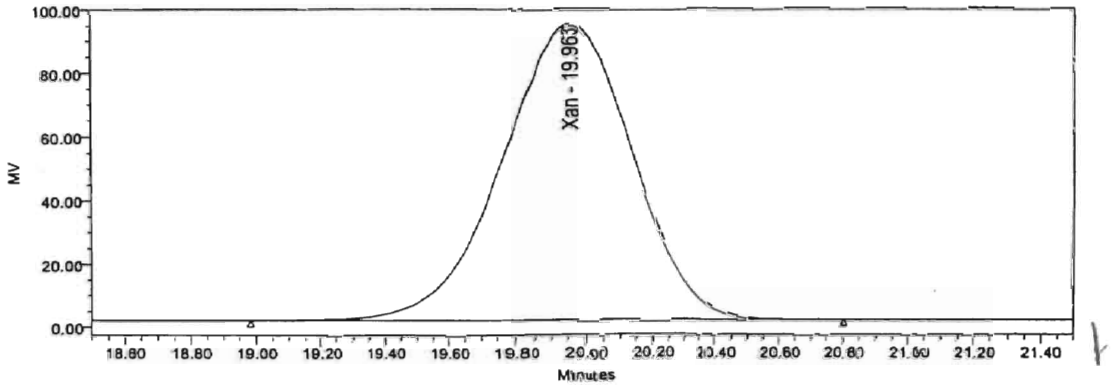

	RT	% Area	Area	Width (sec)	Height	Units	Baseline Start (min)
1	19.963	100.00	2479802	109.000	93371	micro gm	19.583

	Baseline End (min)	Offset (µV)	Slope (µV/sec)
1	20.800	2.001772e+000	7.729845e-003

Sample Report

Reported by User: System

Project Name: XanthanJan92003

SAMPLE INFORMATION

Sample Name:	C05S30	Acquired By:	System
Sample Type:	Unknown	Date Acquired:	2/5/2003 8:10:24 PM
Vial:	90	Acq. Method Set:	Xanthan New
Injection #:	1	Date Processed:	2/7/2003 3:53:27 PM
Injection Volume:	100.00 ul	Processing Method:	Xanthan Calibration Final
Run Time:	25.0 Minutes	Channel Name:	410
Sample Set Name:	XanFeb03	Proc. Chnl. Descr.:	

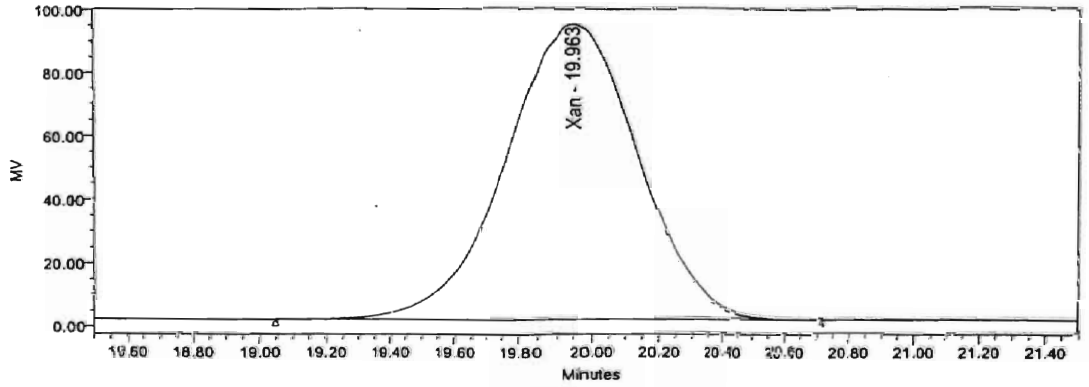

	RT	% Area	Area	Width (sec)	Height	Units	Baseline Start (min)
1	19.963	100.00	2481675	100.000	93344	micro gm	19.050

	Baseline End (min)	Offset (µV)	Slope (µV/sec)
1	20.717	2.479540e+000	-1.123404e-002

Sample Report

Reported by User: System

Project Name: XanthanJan92003

SAMPLE INFORMATION

Sample Name:	C10S0	Acquired By:	System
Sample Type:	Unknown	Date Acquired:	2/5/2003 8:36:50 PM
Vial:	91	Acq. Method Set:	Xanthan New
Injection #:	1	Date Processed:	2/7/2003 3:33:27 PM
Injection Volume:	100.00 ul	Processing Method:	Xanthan Calibration Final
Run Time:	25.0 Minutes	Channel Name:	410
Sample Set Name:	XanFeb03	Proc. Chnl. Descr.:	

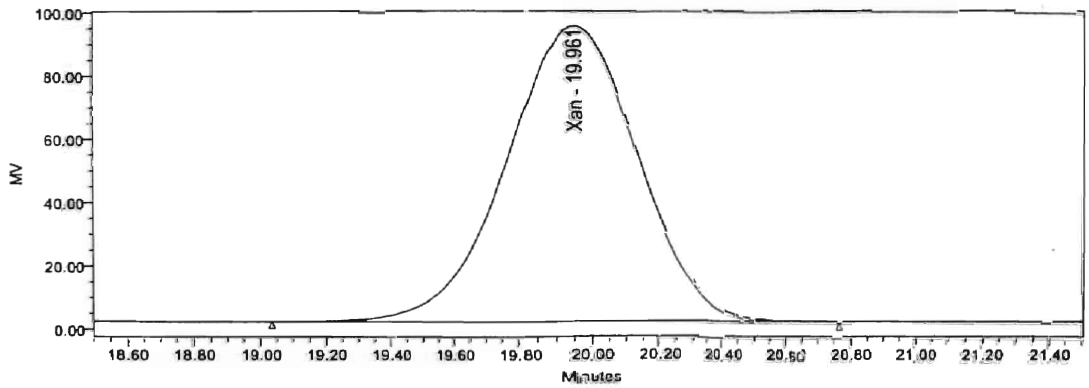

	RT	% Area	Area	Width (sec)	Height	Units	Baseline Start (min)
1	19.961	100.00	2483077	104.000	93411	micro gm	19.033

	Baseline End (min)	Offset (µV)	Slope (µV/sec)
1	20.767	2.989894e+000	-3.510638e-002

Sample Report

Reported by User: System

Project Name: XanthanJan92003

SAMPLE INFORMATION

Sample Name:	C10S5	Acquired By:	System
Sample Type:	Unknown	Date Acquired:	2/5/2003 9:03:15 PM
Vial:	92	Acq. Method Set:	Xanthan New
Injection #:	1	Date Processed:	2/7/2003 3:53:27 PM
Injection Volume:	100.00 ul	Processing Method:	Xanthan Calibration Final
Run Time:	25.0 Minutes	Channel Name:	410
Sample Set Name:	XanFeb03	Proc. Chnl. Descr.:	

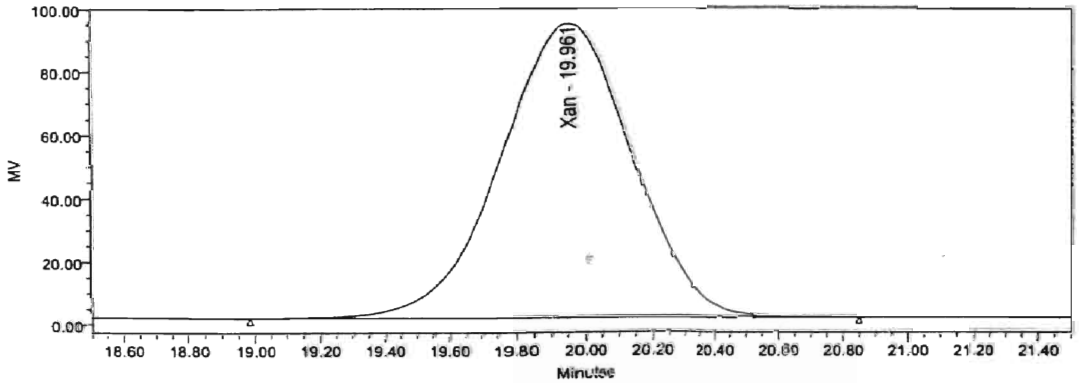

	RT	% Area	Area	Width (sec)	Height	Units	Baseline Start (min)
1	19.961	100.00	2482541	112.000	93255	micro gm	18.983

	Baseline End (min)	Offset (µV)	Slope (µV/sec)
1	20.850	8.764894e-001	7.021277e-002

Sample Report

Reported by User: System

Project Name: XanthanJan92003

SAMPLE INFORMATION

Sample Name:	C10S10	Acquired By:	System
Sample Type:	Unknown	Date Acquired:	2/5/2003 9:29:40 PM
Vial:	93	Acq. Method Set	Xanthan New
Injection #:	1	Date Processed:	2/7/2003 3:53:27 PM
Injection Volume:	100.00 ul	Processing Method:	Xanthan Calibration Final
Run Time:	25.0 Minutes	Channel Name:	410
Sample Set Name:	XanFeb03	Proc. Chnl. Descr.:	

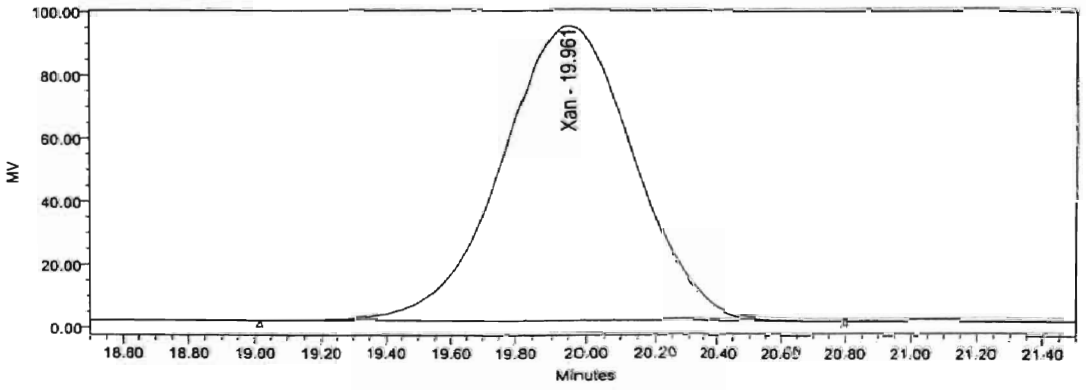

	RT	% Area	Area	Width (sec)	Height	Units	Baseline Start (min)
1	19.961	100.00	2485541	107.000	93388	micro gm	19.017

	Baseline End (min)	Offset (µV)	Slope (µV/sec)
1	20.800	2.349787e+000	0.000000e+000

Sample Report

Reported by User: System

Project Name: XanthanJan92003

SAMPLE INFORMATION

Sample Name:	C10S15	Acquired By:	System
Sample Type:	Unknown	Date Acquired:	2/5/2003 9:56:05 PM
Vial:	94	Acq. Method Set:	Xanthan New
Injection #:	1	Date Processed:	2/7/2003 3:53:27 PM
Injection Volume:	100.00 ul	Processing Method:	Xanthan Calibration Final
Run Time:	25.0 Minutes	Channel Name:	410
Sample Set Name:	XanFeb03	Proc. Chnl. Descr.:	

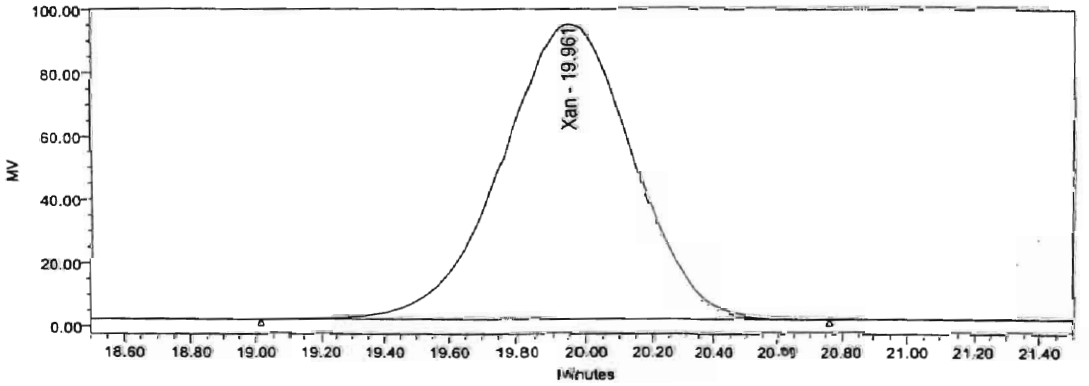

	RT	% Area	Area	Width (sec)	Height	Units	Baseline Start (min)
1	19.961	100.00	2481698	105.000	93347	micro gm	19.017

	Baseline End (min)	Offset (µV)	Slope (µV/sec)
1	20.767	3.015716e+000	-3.477204e-002

Sample Report

Reported by User: System

Project Name: XanthanJan92003

SAMPLE INFORMATION

Sample Name:	C10S30	Acquired By:	System
Sample Type:	Unknown	Date Acquired:	2/5/2003 10:22:30 PM
Vial:	95	Acq. Method Set:	Xanthan New
Injection #:	1	Date Processed:	2/7/2003 3:53:27 PM
Injection Volume:	100.00 ul	Processing Method:	Xanthan Calibration Final
Run Time:	25.0 Minutes	Channel Name:	410
Sample Set Name:	XanFeb03	Proc. Chnl. Descr.:	

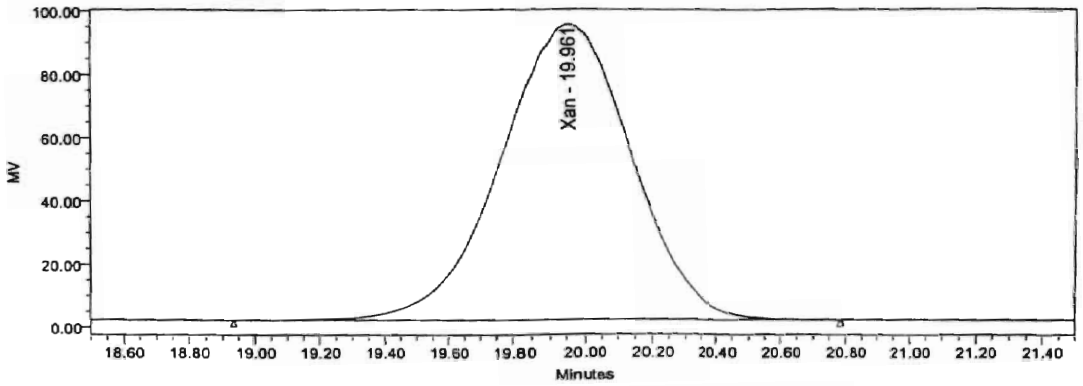

	RT	% Area	Area	Width (sec)	Height	Units	Baseline Start (min)
1	19.961	100.00	2489356	111.000	93488	micro gm	18.933

	Baseline End (min)	Offset (µV)	Slope (µV/sec)
1	20.783	2.480556e+000	-1.012076e-002

Sample Report

Reported by User: System

Project Name: XanthanJan92003

SAMPLE INFORMATION

Sample Name:	C1	Acquired By:	System
Sample Type:	Unknown	Date Acquired:	2/4/2003 7:19:26 PM
Vial:	43	Acq. Method Set:	Xanthan New
Injection #:	1	Date Processed:	2/7/2003 3:53:30 PM
Injection Volume:	100.00 ul	Processing Method:	Xanthan Calibration Final
Run Time:	25.0 Minutes	Channel Name:	410
Sample Set Name:	XanFeb04_12PM	Proc. Chnl. Descr.:	

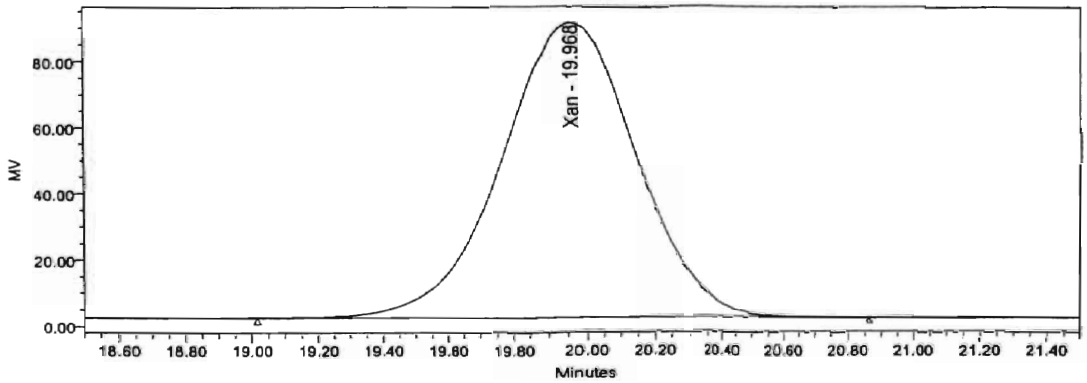

	RT	% Area	Area	Width (sec)	Height	Units	Baseline Start (min)
1	19.968	100.00	2386068	111.000	89267	micro gm	19.017

	Baseline End (min)	Offset (µV)	Slope (µV/sec)
1	20.867	2.602553e+000	0.000000e+000

Sample Report

Reported by User: System

Project Name: XanthanJan92003

SAMPLE INFORMATION

Sample Name:	MB1	Acquired By:	System
Sample Type:	Unknown	Date Acquired:	2/4/2003 7:50:42 PM
Vial:	44	Acq. Method Set:	Xanthan New
Injection #:	1	Date Processed:	2/7/2003 3:53:30 PM
Injection Volume:	100.00 ul	Processing Method:	Xanthan Calibration Final
Run Time:	25.0 Minutes	Channel Name:	410
Sample Set Name:	XanFeb04_12PM	Proc. Chnl. Descr.:	

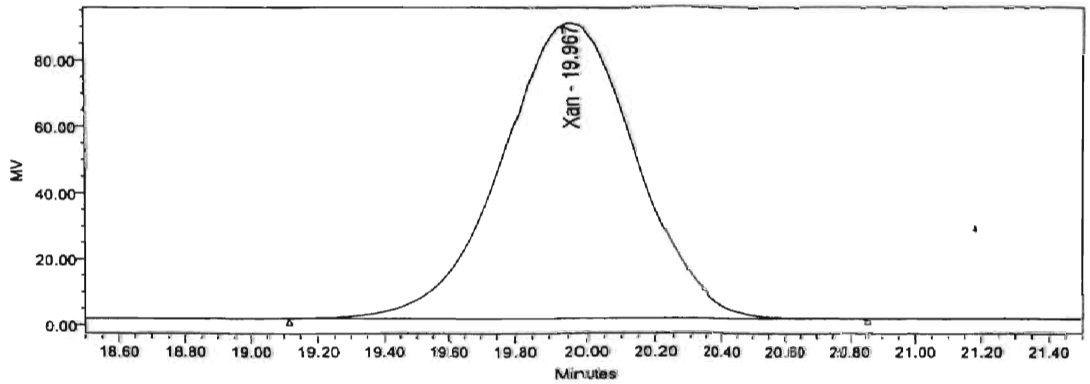

	RT	% Area	Area	Width (sec)	Height	Units	Baseline Start (min)
1	19.967	100.00	2383569	104.000	89219	micro gm	19.117

	Baseline End (min)	Offset (µV)	Slope (µV/sec)
1	20.850	2.908969e+000	-4.320786e-002

Sample Report

Reported by User: System

Project Name: XanthanJan92003

SAMPLE INFORMATION

Sample Name:	C2	Acquired By:	System
Sample Type:	Unknown	Date Acquired:	2/4/2003 8:21:56 PM
Vial:	45	Acq. Method Set:	Xanthan New
Injection #:	1	Date Processed:	2/7/2003 3:53:30 PM
Injection Volume:	100.00 ul	Processing Method:	Xanthan Calibration Final
Run Time:	25.0 Minutes	Channel Name:	410
Sample Set Name:	XanFeb04_12PM	Proc. Chnl. Descr.:	

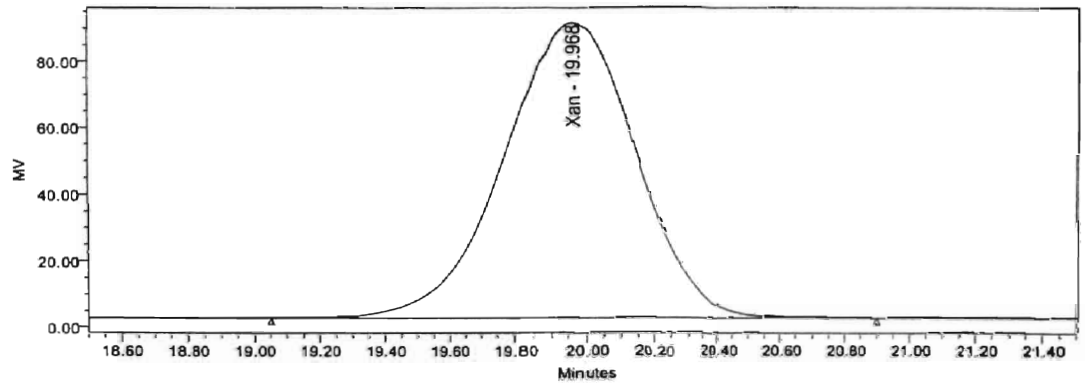

	RT	% Area	Area	Width (sec)	Height	Units	Baseline Start (min)
1	19.968	100.00	2374212	111.000	889113	micro gm	19.050

	Baseline End (min)	Offset (µV)	Slope (µV/sec)
1	20.900	2.105624e+000	3.542266e-002

Sample Report

Reported by User: System

Project Name: XanthanJan92003

SAMPLE INFORMATION

Sample Name:	MB2	Acquired By:	System
Sample Type:	Unknown	Date Acquired:	2/4/2003 8:53:10 PM
Vial:	46	Acq. Method Set:	Xanthan New
Injection #:	1	Date Processed:	2/7/2003 3:53:30 PM
Injection Volume:	100.00 ul	Processing Method:	Xanthan Calibration Final
Run Time:	25.0 Minutes	Channel Name:	410
Sample Set Name:	XanFeb04_12PM	Proc. Chnl. Descr.:	

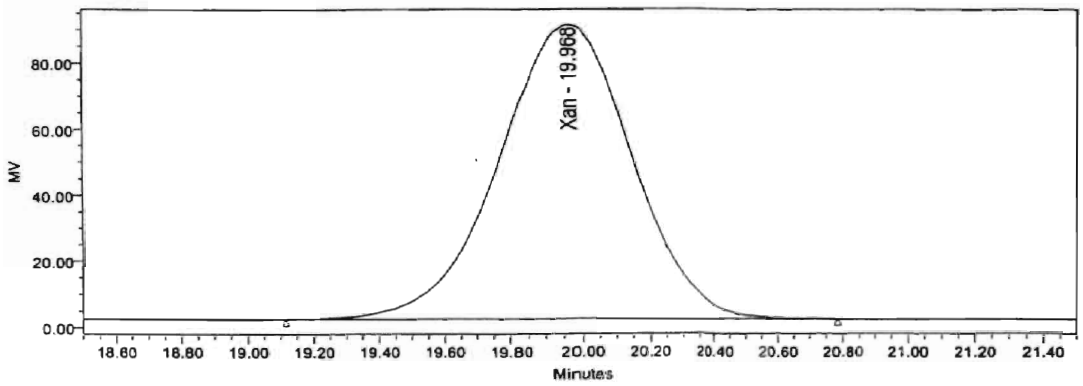

	RT	% Area	Area	Width (sec)	Height	Units	Baseline Start (min)
1	19.968	100.00	2373184	100.000	89035	micro gm	19.117

	Baseline End (min)	Offset (µV)	Slope (µV/sec)
1	20.783	2.684328e+000	-2.808511e-003

APPENDIX.A.15. Blow up of Dissolved oxygen profile during microbubble substitution

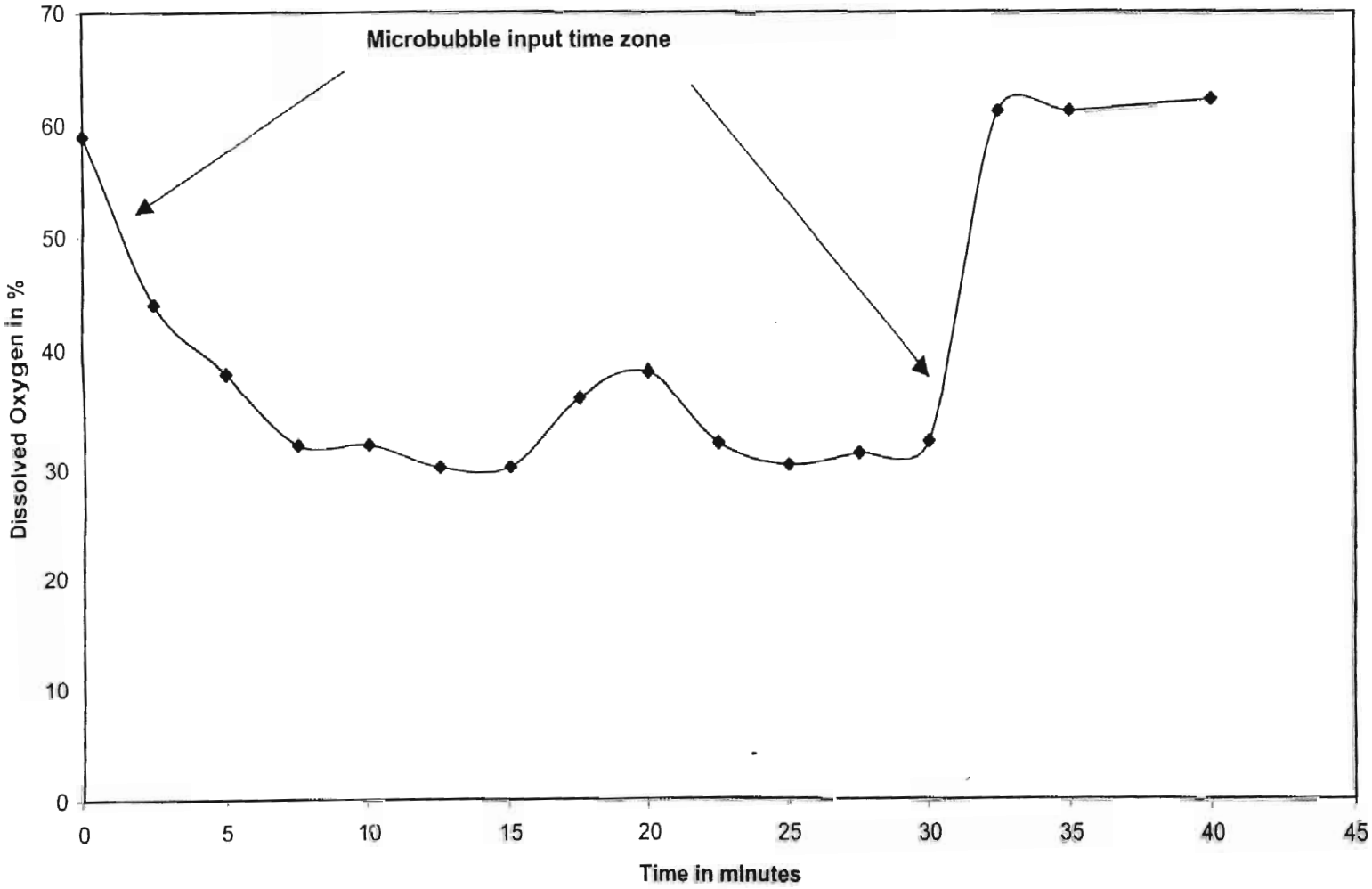

VITA

BANGALORE DHARMENDRA

Candidate for the Degree of

Master of Science

Thesis: UTILIZATION OF MICROBUBBLES FOR ENHANCEMENT OF OXYGEN TRANSFER IN XANTHAN FERMENTATION

Major: Biosystems Engineering

Biographical:

Personal: Born in Bangalore, India. On May 28, 1975, the son of T.K. Vijiyendranathan and B.T.Rathna

Education: Graduated from KLE College, Bangalore, India in May 1992; received Bachelor of Technology degree in Dairy Technology from UAS, Bangalore, India in November 1996; and a Masters of Technology in Dairy Engineering from National Dairy Research Institute, Karnal, India in May 2000, respectively. Completed the requirements for the Masters of Science degree with a major in Biosystems Engineering at Oklahoma State University, Stillwater, Oklahoma in August '03.

Experience: Employed by Bangalore Dairy and Tropical Fruit International for internship from 1995-1996; Employed by National Dairy Research Institute as a Research Assistant, India from 1997-2000; Employed by Glaxo-Smithkline as Executive Manager-Operations, India from 2000-2001; Employed by the Biosystems and Agricultural Engineering Department at Oklahoma State University in Stillwater, Oklahoma as a Research assistant, 2001-present.

Professional Memberships: Institute of Food Technologists, American Society of Agricultural Engineers, Phi Kappa Phi & Alpha Epsilon